RESEARCH PAPER

Mathematical analysis of Ebola considering transmission at treatment centres and survivor relapse using fractal-fractional Caputo derivatives in Uganda

Isaac Kwasi Adu (ID) [1,*,‡], **Fredrick Asenso Wireko** (ID) [2,‡], **Samuel Akwasi Adarkwa** (ID) [3,‡] **and Gerald Ohene Agyekum** (ID) [3,‡]

[1]Department of Mathematical Sciences, Faculty of Applied Sciences and Technology, Kumasi Technical University, 854, Kumasi, Ghana, [2]Department of Mathematics, College of Science, Kwame Nkrumah University of Science and Technology, 854, Kumasi, Ghana, [3]Department of Statistical Sciences, Faculty of Applied Sciences and Technology, Kumasi Technical University, 854, Kumasi, Ghana

* Corresponding Author
‡ isaac.kadu@kstu.edu.gh (Isaac Kwasi Adu); fredrick.wireko@knust.edu.gh (Fredrick Asenso Wireko); saadarkwa@gmail.com (Samuel Akwasi Adarkwa); geraldagyekum45@gmail.com (Gerald Ohene Agyekum)

Abstract

In this article, we seek to formulate a robust mathematical model to study the Ebola disease through fractal-fractional operators. The study thus incorporates the transmission rate in the treatment centers and the relapse rate, since the Ebola virus persists or mostly hides in the immunologically protected sites of survivors. The Ebola virus disease (EVD) is one of the infectious diseases that has recorded a high death rate in countries where it is endemic, and Uganda is not an exception. The world at large has suffered from this deadly disease since 1976 when it was declared epidemic by the World Health Organization. The study employed fractal-fractional operators to identify the epidemiological patterns of EVD, especially in treatment centers and relapse. Memory loss and relapse are mostly observed in EVD survivors and this justifies the use of fractional operators to capture the true dynamics of the disease. Through dynamical analysis, the model is proven to be positive and bounded in the region. The model is further explicitly shown to have a solution that is unique and stable. The reproduction number was duly computed by using the next-generation matrix approach. By taking EVD epidemic cases in Uganda, the study fitted all parameters to real data. It has been shown through sensitivity index analysis that the transmission rate outside treatment centers and relapse have a significant effect on the endemic state of the disease, as they lead to an increase in the basic reproduction ratio.

Keywords: Ebola; EVD transmission; Caputo derivatives; numerical simulations; Hyers-Ulam stability
AMS 2020 Classification: 34-02; 34A34; 92B05; 70-10; 34L30

1   Introduction

The Ebola virus is the source of the highly infectious and often fatal disease known as Ebola virus disease (EVD) [1]. The most typical ways of transmitting the Ebola virus to individuals are via direct interaction with secretions, organs, blood, or additional body fluids of an infected person, in addition to interaction with surfaces and items (clothes and bedding) stained with these fluids. Wild animals, including fruit bats, porcupines, and nonhuman primates, are the main carriers of the disease to people. On average, 50% of cases of EVD result in death. Case death rates have varied from 25% to 90% in prior epidemics [1, 2]. Several epidemics of EVD are initiated by a single overflow event and spread from person to person via intimate interactions, often in remote, densely forested locations. Index cases are often associated with hunting, forest work, or land modification.

Infected individuals can spread the virus to other individuals directly, but close contacts such as family members, caregivers, or medical professionals are at more risk of contracting the disease [3]. For instance, the 2014–2015 West Africa Ebola outbreak claimed 109 lives among healthcare professionals in Guinea, sparking alarm worldwide and subsequent instances in Spain and the US. Ebola Rehabilitation Facility for Medical Personnel in Conakry, Guinea, diagnoses and treats healthcare professionals who are infected (either confirmed or suspected) with EVD and are provided with comprehensive medical care, such as biologic monitoring and blood transfusions [4]. The early symptoms of an Ebola infection are fever, myalgia, and asthenia, progressing to gastrointestinal syndrome, including vomiting and diarrhoea. Subsequently, shock, hypoperfusion, failure of several organs, such as serious kidney damage, and depletion of intravenous fluid may occur. Haemorrhage syndrome, primarily gastrointestinal bleeding, may also occur [5]. Furthermore, an Ebola infection may result in several neurological problems. These comprise tremors, migraines, loss of memory, epilepsy, and anomalies of the cranial nerves [6]. Studies have shown that either waning of immunity or weak immunity can lead to virus reinfection in Ebola victims. Some survivors' immunity declines after recovery, while stronger immune systems experience subclinical or asymptomatic sickness [7, 8]. In 2014, during the West African Ebola outbreak, thousands of people survived. It has been reported that the Ebola virus may relapse and cause a potentially fatal and spreadable illness since survivors can harbour the infection for months in immune-privileged sites like the brain, the testes, the central nervous system, and the eyes [6, 8].

In 1976, the world recorded two significant EVD epidemics in South Sudan and also DR Congo (DRC), which led to the initial recognition of the disease worldwide. From that period, countries like DR Congo (DRC) in 1994 and Uganda in 1995 experienced another Ebola outbreak. Ebola outbreaks following this, outbreaks have been reported often and widely in Nigeria, Gabon, the DR Congo, Guinea, Uganda, Liberia, and Sierra Leone. Additionally, rare outbreaks of EVD have been reported from South Africa, the USA, Italy, and the United Kingdom [9].

Recently, mathematical modelling has come to be seen as an important and valuable instrument for understanding the behaviour and cause of the spread of many prevalent infectious diseases, such as diabetes mellitus [10], Ebola [1], measles [11], monkey pox [12], COVID-19 [13], diarrhoea [14], and query fever [15] as stated in [1, 10]. It can also be employed to demonstrate the effective way to mitigate disease propagation and assist in making decisions during an outbreak of disease [1]. For instance, [14] employed Ghana's Ministry of Health data to validate an epidemiological model for diarrhoea transmission dynamics from 2008-2018. They concluded that reducing transmission rates and increasing treatment can significantly control or eradicate the disease. [16], analysed the Hepatitis E model's dynamics and optimal control analysis using the Atangana-Baleanu derivative. When their reproduction number is below one, their model becomes locally asymptotically stable.

They formulated an optimal control system using appropriate control strategies. Numerical results suggest the proper application of control strategies for early Hepatitis E elimination. The Atangana-Baleanu derivative allows for disease status monitoring and effective strategies. A mathematical model predicting giardiasis spread that considers carriers, preventative measures, and interaction between humans and the environment was proposed by [17].

The model uses the Lyapunov function, Metzler constancy hypothesis, and advanced next-generation matrix. Implementing solutions in endemic areas effectively stops giardiasis spread. [18], proposed an article to review malaria biology, mathematical modelling methods, uncertainties, and controversies, and provides a timeline from Ross and MacDonald's classical works to recent climate-focused studies, contextualising mathematical work within the "million-murdering death" of malaria. [19], conducted a pneumonia and HIV/AIDS deterministic co-infection model and used it to assess the impact of these diseases on each other. Their model includes sub-models and sensitivity analysis, revealing that the spreading rate of HIV and the treatment rates are the most sensitive parameters. Their model incorporated intervention strategies and numerical simulations, which shown that prevention and treatment of both diseases reduce the co-infection burden. For more articles on the application of mathematical modelling to study infectious diseases, see [20, 21].

Now, we concentrate on some mathematical models of EVD that have been published earlier by different authors. A nonlinear mathematical model for Ebola was published in 2024 by [1], with an emphasis on burial practices and environmental contamination. They determine the reproduction number, Ebola-free, and Ebola-present equilibrium, as well as the boundedness, positivity, and well-posedness of the model. The sensitivity analysis reveals forward bifurcation, suggesting suppression of Ebola spread. Control strategies include reducing contact with infected people, educating the public, vaccinating the susceptible, and promoting education against funeral customs. Personal protection, vaccination, and safe burial are the most cost-effective methods. In the research of [22], they presented an Ebola virus disease model built using a novel exponentially nonlinear incidence function, which incorporates the curtailment in disease spread as a result of human behaviour. The steady states of the model were determined, and the model's global stability was demonstrated using Lyapunov functions. Their results indicate a good fit when effectiveness and the rate of change of behaviour are faster, after fitting the model to Liberia and Sierra Leone's Ebola data.

In another study, [23], developed an article to explore the dynamics of EVD in domestic and wild animals. They employ an SEIR-type model developed to study the virus's stability in the human population. Their model comprises a nonlinear coupled differential equation, determining Ebola-free and present equilibrium states. The model is asymptotically stable, and global stabilities are carried out using Lyapunov functions theory. The Runge-Kutta method and non-standard finite difference scheme are used for the SEIR model. They concluded that compared to RK4, the NSFD numerical approach is more dependable, preserving non-negativity and boundedness for different step sizes. State-variable simulations provided a numerical analysis of their disease model.

Further, authors of [24] developed a SIR-type model to study Ebola virus disease (EVD) spread using conformable derivatives. Their model incorporates direct and indirect transmission methods, including funeral practices, tainted bush meat consumption, and environmental contamination. The model also considers the possibility of infected individuals birthing and migrating to the existing population. According to their research, the only state in which there is no sickness is when there is no environmental spread of the Ebola virus. In addition, authors of [25] presented a model on the Ebola virus disease. Their model employed mathematical models to understand the spread of the virus validated a new model incorporating vaccination and applied optimal control

analysis to study its impact on numerous shooting techniques with direct multiple shooting methods. Their numerical simulations indicate that an optimal control strategy implemented significantly reduces the number of people prone to Ebola and Ebola-infected people and increases the number of people who recover.

Notwithstanding this, the Ebola virus disease is known to be deadly as it leaves the survivor with severe neurological effects such as seizures, cranial nerve disorders, and memory loss. Authors of [2] presented a mathematical model to explain the dynamics of Ebola transmission between humans and dogs through fractional operators. Caputo-Fabrizio derivative served as the foundation for their model. Fractional orders were shown to have a considerable influence on the model when it was fitted to Uganda's reported Ebola outbreak. According to them, Controlling the spread of Ebola can be achieved by improving recovery rates and decreasing contact rates between dog compartments. They concluded that it is advisable to implement quarantine procedures to regulate encounters during outbreaks. In [26], the Grunwald-Letnikov fractional operator was applied to study the Ebola disease physical patterns in the population, and in [27], the Atangana-Baleanu Caputo operator was also applied to investigate the outbreak of the contagious Ebola disease.

Our motivation for the current research is that all the related literature discussed considers Ebola spreads and how to mitigate the infection. However, we observed that none of the articles examined the following: transmission of Ebola virus disease at treatment centres; Ebola virus persistent in the immunologically protected sites of survivors' bodies and the associated relapse-symptomatic infection; the application of susceptible, infected, treatment and recovered, SITR-type model to investigate the dynamics of Ebola Virus Disease (EVD). Although the authors of [28] employed SITR-type to examine their Ebola model, there are some limitations to their research. These include the use of some parameter values based on assumptions and parameters from existing literature instead of using real Ebola data to carry out their analysis. There are several neurological side effects linked to Ebola. This includes seizures and loss of memory. The memory effect is a crucial characteristic of biological systems. The use of fractional-order models allowed for the realisation of this [6, 29–31]; however, the deterministic approach that was employed in their research was unable to do that. The current research seeks to address these gaps by:

  i. Studying the dynamics of EVD transmission at the treatment centres,
 ii. Incorporating the dynamics of relapse in survivors due to virus persistence in their bodies after recovery,
iii. Applying the least square estimation technique to fit all the model parameters to real data from Uganda,
 iv. Employing the novel fractal-fractional Caputo derivative to capture the exact dynamics of EVD in the population.

The remaining sections of the article are categorised in this pattern. Section 2 deals with formulating the Ebola model that incorporates transmission dynamics at the treatment centres and the relapse patterns in survived individuals. The basic or preliminary results are presented in Section 3. In Section 4, we investigate the positivity and boundedness of the Ebola model understudy. The Ebola model is now studied through fractal-fractional Caputo operators in Section 5 where we performed thorough existence and uniqueness analysis through the fixed point theorem. Also, the Hyers-Ulam and Hyers-Ulam-Rassias stability criterion is used to establish that the Ebola model is stable and is discussed here. Again, we subjected the Ebola model to real data to estimate all the parameters of the study in Section 6, whereas Section 7 performs the local stability analysis and also measures the fundamental reproduction number. In Section 8, the sensitivity analysis of the model's parameters to the R_0 is discussed. Finally, the numerical simulations and conclusion of

the research study are discussed in Section 9 and Section 10, respectively.

2 Ebola model formulation

We propose an integer Ebola transmission model in this section. The entire population is classified into four classes: Susceptible $S(t)$, these are people who are prone to contracting Ebola disease. Infected $I(t)$ are those actively infected with Ebola, show clinical symptoms, and can spread the disease to other individuals. Treated $T(t)$, these are individuals who have received treatment after infection from Ebola. Some individuals of the treated class can still transmit Ebola diseases to other people through direct or indirect means due to the waning of Ebola virus antibodies after a few years of recovery [32]. People who have recovered from the Ebola infection are denoted by $R(t)$. The natural mortality rate is denoted by μ. β is the transmission rate from the infectious class to the treatment class, δ_1 is the Ebola-induced death rate of individuals, and k is the relapse rate of individuals under treatment. The recruitment rate is given by ψ. α_1 is the transfer rate of susceptible to infectious class. α_2 is the transmission rate of partially recovered individuals at the treatment centres to caregivers, σ_1 is the immunity loss rate, and σ_2 denotes the recovery rate. Hence, the entire populace is denoted by $N = S + I + T + R$. The assumptions below formed the basis of the development of the Ebola model:

i. Ebola can spread to susceptible people via any of the following ways: having interpersonal relationships with recovered Ebola victims, touching contaminated animals, or coming into contact with the bodily fluids and clothing of an infected individual,

ii. Recovered individuals can become susceptible to Ebola infection after recovery,

iii. Recovered individuals can transmit Ebola to other people within a few years after recovery due to waning immunity,

The following four (4) integer-order differential equations were developed using the assumptions as basis. The model equations are therefore given by

$$
\begin{aligned}
\frac{dS}{dt} &= \psi + \sigma_1 R(t) - \alpha_1 S(t) I(t) - \mu S(t), \\
\frac{dI}{dt} &= \alpha_1 S(t) I(t) + k T(t) - \alpha_2 I(t) R(t) - (\beta + \delta_1 + \mu) I(t), \\
\frac{dT}{dt} &= \alpha_2 I(t) R(t) + \beta I(t) - (\mu + k + \sigma_2) T(t), \\
\frac{dR}{dt} &= \sigma_2 T(t) - (\sigma_1 + \mu) R(t),
\end{aligned}
\tag{1}
$$

with initial conditions $S(0) = S_0 > 0$, $I(0) = I_0 \geq 0$, $T(0) = T_0 \geq 0$, and $R(0) = R_0 \geq 0$.

3 Preliminary results

In this section, the studies highlight some essential definitions regarding the dynamical analysis to be carried out on the Caputo fractal-fractional Ebola disease model. The definitions are stated below based on literature [33–35].

Definition 1 *Let us suppose there is a continuous domain $(\mathcal{A}, \mathcal{E})$, and further assume that $\mathcal{H}$ has a derivative existing in the fractal dimension range Φ_2. Then, the Caputo fractal-fractional differential operator of $\mathcal{H}$ with the fractional order Φ_1 is given as*

$$
{}^{\mathcal{FFC}}\mathfrak{D}_{\mathcal{A},\mathcal{E}}^{\Phi_1,\Phi_2} \mathcal{H}(\mathcal{E}) = \frac{1}{\Gamma(q - \Phi_1)} \frac{d}{d\mathcal{E}^{\Phi_2}} \int_{\mathcal{A}}^{\mathcal{E}} (\mathcal{E} - k)^{q - \Phi_1 - 1} \mathcal{H}(k) dk, \quad (q - 1 < \Phi_1, \Phi_2 \leq q \in \mathbb{N}),
$$

following differentiation results;

$$\frac{d\mathcal{H}(k)}{dk^{\Phi_2}} = \lim_{\mathcal{E} \to k} \frac{\mathcal{H}(\mathcal{E}) - \mathcal{H}(k)}{\mathcal{E}^{\Phi_2} - k^{\Phi_2}}.$$

By supposing that $\Phi_2 = 1$, then the Caputo fractal-fractional derivative ${}^{\mathcal{FFC}}\mathfrak{D}_{\mathcal{G},\mathcal{E}}^{\Phi_1,\Phi_2}$ yields Φ_1^{th}-Riemann-Liouville derivative ${}^{\mathbf{RL}}\mathfrak{D}_{\mathcal{G},\mathcal{E}}^{\Phi_1}$.

Definition 2 *If we further assume that the map $\mathcal{H}$ is unperturbed in the neighborhood of the open interval $(\mathcal{A}, \mathcal{E})$. Then, it is obvious that the Caputo fractal-fractional integral of $\mathcal{H}$ results in*

$$^{\mathcal{FFC}}\mathfrak{J}_{\mathcal{A},\mathcal{E}}^{\Phi_1,\Phi_2}\mathcal{H}(\mathcal{E}) = \frac{\Phi_2}{\Gamma(\Phi_1)} \int_{\mathcal{A}}^{\mathcal{E}} k^{\Phi_2-1}(\mathcal{E}-k)^{\Phi_1-1}\mathcal{H}(k)dk.$$

By classifying $\mathfrak{A}$ t be a non-decreasing transformation, that is $b : \mathcal{R}_{\geq 0} \to \mathcal{R}_{\geq 0}$ with $b(\mathcal{E}) < \mathcal{E}, \forall \mathcal{E} > 0,$

$$\sum_{u=1}^{\infty} a^u(\mathcal{E}) < \infty.$$

Definition 3 *Let us define the map $\mathcal{H} : \mathbb{V} \to \mathbb{V}$ and $\psi : \mathbb{V}^2 \to \mathcal{R}_{\geq 0}$, with $\mathbb{V}$ to be a normed linear space. We then have*

   i. *In the case where each $x_1, x_2 \in \mathbb{V}$,*

$$\phi(x_1, x_2)\mathbf{d}(\mathcal{H}x_1, \mathcal{H}x_2) < a(d(x_1, x_2)),$$

   then $\mathcal{H}$ is $\psi - a$-contraction,
   ii. *Also, assuming $\psi(x_1, x_2) \geq 1$ yields $\psi(\mathcal{H}x_1, \mathcal{H}x_2) \geq 1$, we have that $\mathcal{H}$ is ψ - admissible.*

4 Positivity and boundedness

This section establishes the positivity and boundedness of solutions to the proposed Ebola model. By following a similar procedure as performed in literature [20], we obtain the positivity and boundedness of the Ebola model in this manner.

Positivity of solutions

To establish the positivity of the model's solutions, we show that the solutions to each equation of the model are non-negative for any $t > 0$. Let us begin the proof by first supposing that $S(t)$ and $I(t)$ possess the same signs and $\alpha_1 > 0$. In this manner, we suppose that the following inequality holds for $T(t)$ compartment,

$$T(t) \geq T_0 e^{-(\mu+k+\sigma_2)}, \quad \forall t > 0.$$

Noting from the above that $T(t)$ is positive, it suffices that

$$I = \alpha_1 SI + kT - \alpha_2 IR - (\beta + \delta_1 + \mu)I$$
$$\geq -(\beta + \delta_1 + \mu)I.$$

Thus, we have

$$I \geq I_0 e^{-(\beta + \delta_1 + \mu)}.$$

Subsequently, by following the same approach, we have

$$R \geq R_0 e^{-(\sigma_1 + \mu)}.$$

Now, let us suppose that the $I(t)$ and $T(t)$ compartments are integrable, this implies that the following inequality arises:

$$\mathcal{G}(t) \geq \mathcal{G}_0 + \int [\delta_1 (I + T)] dt, \quad \forall t > 0.$$

Importantly, we explicitly establish the positivity of the $S(t)$ compartment by first supposing the norm below exists: $\|g\| = \sup_{t \in D_g} |g|$. This suffices that for the susceptible compartment, $S(t)$, we have

$$\begin{aligned}
\dot{S}(t) &= \psi + \sigma_1 R - \alpha_1 S I - \mu S \\
&\geq \sigma_1 R - (\alpha_1 I + \mu) S \geq -(\alpha_1 |I| + \mu) S \\
&\geq -(\alpha_1 \sup_{t \in D_g} |I| + \mu) S \geq -(\alpha_1 \|I\|_\infty + \mu) S \\
&\geq -\varphi S,
\end{aligned}$$

where we define

$$\varphi = (\alpha_1 \|I\|_\infty + \mu).$$

Obviously, this yields

$$S(t) = S_0 e^{-\varphi t}.$$

We observe that these results hold for all other compartments. Hence, all the solutions of the Ebola model are positive.

Boundedness of solutions

To prove the boundedness of solutions to the model, we first consider the total human population,

$$N(t) = S(t) + I(t) + T(t) + R(t). \tag{2}$$

Substituting all equations of the model, we obtain,

$$\begin{aligned}
\frac{dN(t)}{dt} &= \frac{dS(t)}{dt} + \frac{dI(t)}{dt} + \frac{dT(t)}{dt} + \frac{dR(t)}{dt} \\
&= \psi + \sigma_1 R(t) - \alpha_1 S(t) I(t) - \mu S(t) + \alpha_1 S(t) I(t) + kT(t) - \alpha_2 I(t) R(t) \\
&\quad - (\beta + \delta_1 + \mu) I(t) + \alpha_2 I(t) R(t) + \beta I(t) - (\mu + k + \sigma_2) T(t) + \sigma_2 T(t) - (\mu + \sigma_1) R(t) \\
&= \psi - \mu N - \delta_1 I(t).
\end{aligned} \tag{3}$$

In the absence of Ebola-related deaths, ($\delta_1 = 0$), we have

$$\frac{dN}{dt} \leq \psi - \mu N. \tag{4}$$

Now taking the Laplace transform of (4), we obtain

$$\begin{aligned}
\mathcal{L}\{N'(t)\} + \mu\mathcal{L}\{N(t)\} &\leq \mathcal{L}\{\psi\}, \\
s\mathcal{N}(s) - N(0) + \mu\mathcal{N}(s) &\leq \frac{\psi}{s}, \\
\mathcal{N}(s) &\leq \frac{\psi}{s(s+\mu)} + \frac{N(0)}{s+\mu}.
\end{aligned} \tag{5}$$

The inverse Laplace of (5) is

$$N(t) \leq \frac{\psi}{\mu}(1 - e^{-\mu t}) + N(0)e^{-\mu t}. \tag{6}$$

Taking the $\limsup_{t\to\infty}$ of the above equation, we get

$$N(t) \leq \frac{\psi}{\mu}. \tag{7}$$

Now, the solutions of the Ebola model are bounded and feasible in the region

$$\mathcal{V} = \left\{ (S, I, T, R) \in \mathbb{R}_+^4 | N \leq \frac{\psi}{\mu} \right\}. \tag{8}$$

5 Caputo fractal-fractional Ebola model

It has been reported in the literature that individuals who have suffered from the Ebola virus disease mostly face severe neurological disorders such as cranial nerve disorders, memory loss, recurring seizures, and others for about six months or more even after recovery [6]. As a result of this, using integer order operator models to study the dynamics of the Ebola disease virus may yield uncertain or unreliable conclusions. In addition, since there occurs mostly structural variability in the dynamics of the Ebola disease, that is, the disease is influenced by physical occurrences, a fractional analysis of the dynamics of the Ebola is the appropriate operator to measure the physical dynamics of the disease [7]. The Caputo fractal-fractional derivative has been chosen for this study due to its enormous advantages over the other fractional operators. For instance, it has been reported in the literature that the Caputo fractal-fractional derivative presents a better description of complex systems, such as biological processes, by accurately measuring these systems' inherent hereditary and memory properties. Again, the Caputo fractal-fractional derivative is quite simplified as it allows the use of standard initial conditions compared to the Riemann-Liouville derivative. As a result, the Caputo fractal-fractional derivative has a minimal computational complexity and requires a minimum storage space when its algorithm is simulated [36–38]. In this study, the Ebola virus disease is thus investigated using the Caputo fractal-fractional operator. From this knowledge, Eq. (1) is reformulated into a non-integer model using Caputo operators in this manner:

$$
\begin{aligned}
{}^{FFC}\mathcal{D}_{0,t}^{\Phi_1,\Phi_2} S(t) &= \psi + \sigma_1 R(t) - \alpha_1 S(t)I(t) - \mu S(t), \\
{}^{FFC}\mathcal{D}_{0,t}^{\Phi_1,\Phi_2} I(t) &= \alpha_1 S(t)I(t) + \kappa T(t) - \alpha_2 I(t)R(t) - (\beta + \delta_1 + \mu)I(t), \\
{}^{FFC}\mathcal{D}_{0,t}^{\Phi_1,\Phi_2} T(t) &= \alpha_2 I(t)R(t)\beta I(t) - (\mu + \kappa + \sigma_2)T(t), \\
{}^{FFC}\mathcal{D}_{0,t}^{\Phi_1,\Phi_2} R(t) &= \sigma_2 T(t) - (\sigma_1 + \mu)R(t),
\end{aligned}
\tag{9}
$$

with initial conditions $S(0) = S_0 > 0$, $I(0) = I_0 \geq 0$, $T(0) = T_0 \geq 0$, and $R(0) = R_0 \geq 0$.

Existence and uniqueness of the Caputo fractal-fractional Ebola disease model

A key aspect of mathematical modelling is to examine if there exists a unique solution for the model under study. To establish that model (9) is injective, a thorough existence and uniqueness analysis is carried out using the fixed point theory as done in literature [39–42]. By supposing that there exists the norm $\mathbf{B}(\tau)$ which is defined to be a Banach space and further assumed to be a continuous real-valued map defined in the domain $\tau(0, T)$ with a defined sub norm. Then we note that there is $\mathcal{G} = \mathbf{B}(\tau_1) \times \mathbf{B}(\tau_2) \times \mathbf{B}(\tau_3) \times \mathbf{B}(\tau_4)$ which is imposed on the norm $\|(S, I, T, R)\| = \|S\| + \|I\| + \|T\| + \|R\|$, where $\|S\| = \sup_{t\in\tau}|S|, \|I\| = \sup_{t\in\tau}|I|, \|T\| = \sup_{t\in\tau}|T|, \|R\| = \sup_{t\in\tau}|R|$. From the suppositions above, the fractal-fractional Ebola disease model in the Caputo sense is reconstructed as;

$$
\begin{aligned}
S(t) - S(0) &= {}^{C}\mathcal{D}_t^{\Phi_1,\Phi_2}\left[\psi + \sigma_1 R(t) - \alpha_1 S(t)I(t) - \mu S(t)\right], \\
I(t) - I(0) &= {}^{C}\mathcal{D}_t^{\Phi_1,\Phi_2}\left[\alpha_1 S(t)I(t) + \kappa T(t) - \alpha_2 I(t)R(t) - (\beta + \delta_1 + \mu)I(t)\right], \\
T(t) - T(0) &= {}^{C}\mathcal{D}_t^{\Phi_1,\Phi_2}\left[\alpha_2 I(t)R(t)\beta I(t) - (\mu + \kappa + \sigma_2)T(t)\right], \\
R(t) - R(0) &= {}^{C}\mathcal{D}_t^{\Phi_1,\Phi_2}\left[\sigma_2 T(t) - (\sigma_1 + \mu)R(t)\right].
\end{aligned}
\tag{10}
$$

For convenient evaluations, the equations in (10) are redefined as,

$$
\begin{cases}
\mathcal{J}_1(S, I, T, R) = \psi + \sigma_1 R(t) - \alpha_1 S(t)I(t) - \mu S(t), \\
\mathcal{J}_2(S, I, T, R) = \alpha_1 S(t)I(t) + \kappa T(t) - \alpha_2 I(t)R(t) - (\beta + \delta_1 + \mu)I(t), \\
\mathcal{J}_3(S, I, T, R) = \alpha_2 I(t)R(t)\beta I(t) - (\mu + \kappa + \sigma_2)T(t), \\
\mathcal{J}_4(S, I, T, R) = \sigma_2 T(t) - (\sigma_1 + \mu)R(t).
\end{cases}
\tag{11}
$$

Now through the Riemann-Liouville integral operator, the fractal-fractional Ebola disease model (9) suffices that;

$$
\begin{aligned}
{}^{RL}\mathcal{D}_t^{\Phi_1} S(t) &= \Phi_{2_*} t^{*\Phi_2 - 1}\mathcal{J}_1(S, I, T, R), \\
{}^{RL}\mathcal{D}_t^{\Phi_1} I(t) &= \Phi_{2_*} t^{*\Phi_2 - 1}\mathcal{J}_2(S, I, T, R), \\
{}^{RL}\mathcal{D}_t^{\Phi_1} T(t) &= \Phi_{2_*} t^{*\Phi_2 - 1}\mathcal{J}_3(S, I, T, R), \\
{}^{RL}\mathcal{D}_t^{\Phi_1} R(t) &= \Phi_{2_*} t^{*\Phi_2 - 1}\mathcal{J}_4(S, I, T, R).
\end{aligned}
\tag{12}
$$

Now in order to solve the model, Eq. (12) is reformulated as an initial value problem

$$
\begin{cases}
{}^{RL}\mathcal{D}_t^{\Phi_1}\mathcal{Q}(t^*) = \Phi_{2_*} t^{*\Phi_2 - 1}\mathcal{J}(t, \mathcal{Q}(t)) \\
\quad \mathcal{Q}(0) = \mathcal{Q}_0, \qquad \Phi_1, \Phi_{2_*} \in (0, 1],
\end{cases}
\tag{13}
$$

where $t^* \in \mathcal{U}$, such that

$$\begin{aligned}
\mathcal{Q}(t^*) &= (S(t^*), I(t^*), T(t^*), R(t^*)), \\
\mathcal{Q}(0) &= (S_0, I_0, T_0, R_0)^t.
\end{aligned}$$ (14)

Also,

$$\mathcal{J}(t, \mathcal{Q}(t)) = \begin{cases}
\mathcal{J}_1(S(t^*), I(t^*), T(t^*), R(t^*)), \\
\mathcal{J}_2(S(t^*), I(t^*), T(t^*), R(t^*)), \\
\mathcal{J}_3(S(t^*), I(t^*), T(t^*), R(t^*)), \\
\mathcal{J}_4(S(t^*), I(t^*), T(t^*), R(t^*)).
\end{cases}$$ (15)

Now by applying the fundamental theorem of calculus to (13), we obtain

$$\mathcal{Q}(t^*) = \mathcal{Q}(0) + \frac{\Phi_{2_*}}{\Gamma(\Phi_1^*)} \int_0^{t^*} \Omega^{*\Phi_{2_*}-1}(t^* - \Omega^*)^{\Phi_1^*-1} \mathcal{J}(\Omega^* \mathcal{Q}(\Omega^*)) h^* \Omega^*,$$ (16)

thus, leading to the following relations:

$$\begin{aligned}
S(t^*) &= S(0) + \frac{\Phi_{2_*}}{\Gamma(\Phi_1^*)} \int_0^{t^*} \Omega^{*\Phi_{2_*}-1}(t^* - \Omega^*)^{\Phi_2^*-1} \mathcal{J}_1 \\
&\quad \times [S(\Omega^*), I(\Omega^*), T(\Omega^*), R(\Omega^*)], \\
I(t^*) &= I(0) + \frac{\Phi_{2_*}}{\Gamma(\Phi_1^*)} \int_0^{t^*} \Omega^{*\Phi_{2_*}-1}(t^* - \Omega^*)^{\Phi_2^*-1} \mathcal{J}_2 \\
&\quad \times [S(\Omega^*), I(\Omega^*), T(\Omega^*), R(\Omega^*)], \\
T(t^*) &= T(0) + \frac{\Phi_{2_*}}{\Gamma(\Phi_1^*)} \int_0^{t^*} \Omega^{*\Phi_{2_*}-1}(t^* - \Omega^*)^{\Phi_2^*-1} \mathcal{J}_3 \\
&\quad \times [S(\Omega^*), I(\Omega^*), T(\Omega^*), R(\Omega^*)], \\
R(t^*) &= R(0) + \frac{\Phi_{2_*}}{\Gamma(\Phi_1^*)} \int_0^{t^*} \Omega^{*\Phi_{2_*}-1}(t^* - \Omega^*)^{\Phi_2^*-1} \mathcal{J}_4 \\
&\quad \times [S(\Omega^*), I(\Omega^*), T(\Omega^*), R(\Omega^*)].
\end{aligned}$$ (17)

Now model (9) is reconstructed as a fixed point problem by using the fixed point theory technique. We initially suppose that the given dual function $\mathcal{W} = \mathcal{H}^* \longrightarrow \mathcal{H}^*$ be defined as

$$\mathcal{W}[\mathcal{Q}(t^*)] = \mathcal{Q}(0) + \frac{\Phi_{2_*}}{\Gamma(\Phi_1)} \int_0^{t^*} \Omega^{*\Phi_{2_*}-1}(t^* - \Omega^*)^{\Phi_1^*-1} \mathcal{J}(\Omega^* \mathcal{Q}(\Omega^*)) h^* \Omega^*.$$ (18)

We explicitly define the fixed point theorem for $\Theta^* - \psi^*$ contractions to suffice our proof.

Theorem 1 ([35]) *Let us suppose a complete metric space is stated such that $\psi^* \in \mathcal{B}, \Theta^* : \mathcal{H}^{*2} \longrightarrow \mathbb{R}$, and $\mathcal{W} : \mathcal{H}^* \longrightarrow H^*$ which is an $\Theta^* - \psi^*$ contraction such that the following properties are valid:*
a. $\mathcal{W}$ is θ^* permissible.
b. We have h_0, which is in the function $\mathcal{H}^*$ such that $\Theta^*(\psi_0^*, \mathcal{W}\psi_0^*) \geq 1$.
c. Supposing that for any $h_{\psi_*}^*$ which is an improper subset of $\mathcal{W}^*$ where $h_{\psi_*}^* \longrightarrow h^*$ and $\Theta^*(h_{\psi_*}^*, h_{\psi_*+1}^*) \geq 1, \forall \psi^* \geq 1$, then there exists $\Theta^*(h_{\psi_*}^*, h^*) \geq 1$ for every $\psi^* \geq 1$.

The proof of the theorem is carried out through $\Theta^* - \psi^*$ contractions.

Theorem 2 *Let us suppose that we have a φ^* such that $\mathcal{R} \times \mathcal{R} \longrightarrow \mathcal{R}$ and also there is an $\psi^* \in \mathcal{B}$ for any given operator $\mathcal{J} \in \mathcal{W}(\mathcal{K} \times \mathcal{H}^*, \mathcal{H}^*)$. Also, B1 for any given $\mathcal{J}_1, \mathcal{J}_2, \mathcal{J}_3, \mathcal{J}_4 \in \mathcal{H}^*$ and there is $t^* \in \mathcal{A}$,*

$$|\mathcal{J}(t^*, \mathcal{Q}_1(t^*) - \mathcal{J}(t^*, \mathcal{Q}_2(t^*))| \leq \Theta^* \vartheta^*(|\mathcal{Q}_1(t^*) - \mathcal{Q}_2(t^*)|),$$

also realising that $\chi^*(\mathcal{Q}_1(t^*), \mathcal{Q}_2(t^*)) \geq 0$ and also $\vartheta^* = \frac{\Gamma(\Phi_{2_*} + \Phi_{1_*})}{\Phi_{2_*} \eta^{\Phi_{2_*} + \Phi_{1_*} - 1} \Gamma(\Phi_{2_*})}$.
G2 Also, for any given $t^* \in \mathcal{A}$ there is a $\mathcal{Q}_0 \in \mathcal{H}^*$ such that

$$a^*(\mathcal{Q}_0(t^*), \mathcal{C}(\mathcal{Q}_0(t^*))) \geq 0,$$

given further that

$$a^*(\mathcal{Q}_1(t^*), \mathcal{Q}_2(t^*)) \geq 0 \longrightarrow a^*(\mathcal{C}(\mathcal{Q}_0(t^*)), \mathcal{C}(\mathcal{Q}_0(t^*))) \geq 0.$$

G3 Supposing that $\{\mathcal{Q}_{\psi^*}\}_{\psi^* \geq 1} \subseteq \mathcal{H}^*$ for $\mathcal{Q}_{n^*} \longrightarrow \mathcal{Q}$, such that

$$a^*(\mathcal{Q}_{\psi^*}(t^*), \mathcal{Q}_{\psi^*+1}(t^*)) \geq 0 \longrightarrow a^*(\mathcal{Q}_{\psi^*}(t^*)), (\mathcal{Q}(t^*)) \geq 0,$$

with any given ψ^* and $t^* \in \mathcal{A}$.
We hereby validate the Caputo fractal-fractional Ebola model to have a solution by the proof below.

Proof Let us suppose that there exists the functions $\mathcal{J}_1, \mathcal{J}_2, \mathcal{J}_3, \mathcal{J}_4 \in \mathcal{H}$ such that $\mathcal{J}_1(t^*), \mathcal{J}_2(t^*), \mathcal{J}_3(t^*), \mathcal{J}_4(t^*)$ are non-negative given any time dimension $t^* \in \mathcal{A}$. Applying some basic mathematical ideas in addition to the beta function yields the following;

$$
\begin{aligned}
|\mathcal{W}(\mathcal{Q}_1(t^*)) - \mathcal{W}(\mathcal{Q}_2(t^*))| &\leq \frac{\Phi_{2_*}}{\Gamma(\Phi_1^*)} \int_0^{t^*} \Omega^{*\phi_{2_*}-1}(t^* - \Omega^*)^{\Phi_1^*-1} \\
&\quad \times |\mathcal{J}(\Omega^* \mathcal{Q}_1(\Omega^*)) - \mathcal{J}(\Omega^* \mathcal{Q}_2(\Omega^*))| d^* \Omega^* \\
&\leq \frac{\Phi_{2_*}}{\Gamma(\Phi_1^*)} \int_0^{t^*} \Omega^{*\Phi_{2_*}-1}(t^* - \Omega^*)^{\Phi_1^*-1} \Theta^* \eta^*(|\mathcal{Q}_1(\Omega^*) - \mathcal{Q}_2(\Omega^*)|) d^* \Omega^* \\
&\leq \frac{\Phi_{2_*} \eta^* \eta^{\Phi_{2_*}+\Phi_{1^*}-1} \mathbb{B}(\Phi_{2_*}, \Phi_{1_*})}{\Gamma(\Phi_{1_*})} \Theta^*(\|\mathcal{Q}_1 - \mathcal{Q}_2\|_{\mathcal{H}^*}) \qquad (19) \\
&\leq \frac{\Phi_{2_*} \eta^{\Phi_{2_*}+\Phi_{1^*}-1} \Gamma(\Phi_{2_*})}{\Gamma(\Phi_{1_*} + \Phi_{1^*})} \eta^* \Theta^*(\|\mathcal{Q}_1 - \mathcal{Q}_2\|_{\mathcal{H}^*}).
\end{aligned}
$$

This suffices that

$$\|\mathcal{W}(\mathcal{Q}_1) - \mathcal{W}(\mathcal{Q}_2)\|_{\mathcal{H}^*} \leq \frac{\Phi_{2_*} \eta^{\Phi_{2_*}+\Phi_{1^*}-1} \Gamma(\Phi_{2_*})}{\Gamma(\Phi_{1_*} + \Phi_{1^*})} \eta^* \Theta^*(\|\mathcal{Q}_1 - \mathcal{Q}_2\|_{\mathcal{H}^*}) = \Theta^*(\|\mathcal{Q}_1 - \mathcal{Q}_2\|_{\mathcal{H}^*}).$$

Supposing further that given any values for $\mathcal{Q}_1, \mathcal{Q}_2 \mathcal{H}^*$, we assume that Θ^* is defined to be $\mathcal{H}^* \times \mathcal{H}^* \longrightarrow [0, \infty)$ as stated in

$$\Theta^*(\mathcal{Q}_1, \mathcal{Q}_2) = \begin{cases} 1, & \text{if } a^*(\mathcal{Q}_1(t^*) \geq 0, \\ 0, & \text{otherwise,} \end{cases} \qquad (20)$$

which suffices that,

$$\mathcal{Q}_1, \mathcal{Q}_2 \in \mathcal{H}^*(\mathcal{W}(\mathcal{Q}_1), \mathcal{W}(\mathcal{Q}_2)) \leq (\mathcal{Q}_1, \mathcal{Q}_2),$$

for any $\mathcal{Q}_1, \mathcal{Q}_2 \in \mathcal{H}^*$.

We hereby establish the function $\mathcal{W}$ to be $\Theta^* - \psi^*$ contraction. Whenever there are $\mathcal{Q}_1, \mathcal{Q}_2 \in \mathcal{H}^*$, we observe that $\mathcal{Q}_1, \mathcal{Q}_2 \in \mathcal{H}^* \geq 1$. Stating explicitly the properties of Θ^*, it implies that $a^*(\mathcal{Q}_1(t^*), \mathcal{Q}_2(t^*))$ as non-negative. Then from (G2), we see that $a^*(\mathcal{W}(\mathcal{Q}_1(t^*)), \mathcal{W}(\mathcal{Q}_2(t^*)))$ is non-negative. Then we have Θ^* implying that $\Theta^*(\mathcal{W}(\mathcal{Q}_1(t^*)), \mathcal{W}(\mathcal{Q}_2(t^*))) \geq 1$. This explicitly suffices that the operator $\mathcal{W}$ is a Θ^* admissible.

We then strongly see that (G2) implies that there exist an $\mathcal{Q}_0 \in \mathcal{H}^*$. This then suffices that $t^*(\mathcal{Q}_0(t^*), \mathcal{W}(\mathcal{Q}_0(t^*)))$ is non-negative for any given t^* in the set $\mathcal{H}$ and

$$\Theta^*(\mathcal{Q}_0, \mathcal{W}(\mathcal{Q}_0)) \geq 1.$$

We can further assume that $\mathcal{Q}_{\psi^* > 1}$ is an improper subset of the set $\mathcal{H}^*$ such that $\mathcal{Q}_{\psi^*}$ has a limit point $\mathcal{Q}$ anytime $\Theta^*(\mathcal{Q}_{\psi^*}, \mathcal{Q}_{\psi^*+1}) \geq 1$. It is explicitly seen in Θ^* that

$$a^*(\mathcal{Q}_{\psi^*}(t^*), \mathcal{Q}_{\psi^*+1}(t^*)) \geq 0.$$

This then suffices from (G3) that $a^*(\mathcal{Q}_{\psi^*}(t^*), \mathcal{Q}(t^*)) \geq 0$, implying further that $\Theta^*(\mathcal{Q}_{\psi^*}(t^*), \mathcal{Q}) \geq 1$ for every given ψ^*. Now from Theorem 1, it is observed that there is an $\mathcal{Q}^* \mathcal{H}^*$ in a manner that $\mathcal{W}(\mathcal{Q}^*) = \mathcal{Q}^*$. This then suffices that $\mathcal{Q}^* = (S^*, I^*, T^*, R^*)^T$ is a solution to the Caputo fractal-fractional Ebola disease model.

Theorem 3 *([43]) By assuming that $\mathcal{H}^*$ is said to be a Banach space, which is a convex function $\mathcal{O}$ which is bounded and closed in $\mathcal{H}^*$, and we have $\alpha \in \mathcal{O}$ which is an open set for $0 \in \alpha$. By defining $\mathcal{P} : \alpha \longrightarrow \mathcal{O}$ to be continuous and compact, then it is either*
a. There exists $b^{**} \in \mathcal{O}$ such that $\mathcal{P}(b^{**}) = b^{**}$, or
b. There is $b^* \in \mu\mathcal{O}$ and $\nu^* \in (0,1)$ such that $\nu^*\mathcal{P}(b^*) = b^*$
should hold.

Remark 1 *Let us define the relation*

$$\Delta = \mathcal{J}_0, \tag{21}$$

and also

$$\circledast = \frac{\Phi_{2_*} \eta^{\Phi_{2_*} + \Phi_{1_*} - 1} \Gamma(\Phi_{2_*})}{\Gamma(\Phi_{2_*} + \Phi_{1_*})}. \tag{22}$$

Theorem 4 *Assuming that the function $\mathcal{J} \in C(\mathbb{Q} \times \mathcal{H}^*, \mathcal{H}^*)$. Then;*
M1: we have $\Theta^* \in \mathcal{N}^1(\mathbb{Q}, \mathbb{R}_+)$ and there have also a non decreasing monotonic function $\mathbb{K} \in C([0, \infty), \mathbb{R}_+)$, implying that for any $t^* \in \mathbb{Q}$ and also $\mathcal{Q} \in \mathcal{H}^*$, we have

$$|\mathcal{J}(t^*), \mathcal{Q}(t^*)| \leq \Theta^*(t^*) \mathbf{G}(|\mathcal{Q}(t^*)|).$$

M1: If there exists $\mathcal{X}$ that is positive and also

$$\frac{\mathcal{X}}{\lambda + \zeta\Theta^*(t^*\mathbf{P}(\mathcal{X}))} > 1,$$

where $\Theta^{**} = \sup_{t^* \in \mathbb{Q}} |\Theta^* t^*|$ and also λ, ζ are defined in Eq. (20) and Eq. (19). We then say that the Caputo fractal-fractional Measles disease model's solution exists.

Proof Let us consider $\mathcal{W} : \mathcal{H}^* \longrightarrow \mathcal{H}^*$ as defined in (18) and

$$\mathcal{N}_\nu = \{\mathcal{Q} \in \mathcal{H}^* : \|\mathcal{Q}\|_{\mathcal{H}^*} \le \nu\}, \forall \delta > 0.$$

Consequently, the operator $\mathcal{W}$ is obtained from the continuous and limited operator $\mathcal{J}$. Then for $\mathcal{Q} \in \mathcal{N}_\nu$ there is;

$$
\begin{aligned}
|\mathcal{W}(\mathcal{Q}(t^*))| &\le |\mathcal{Q}(0)| + \frac{\Phi_{2_*}}{\Gamma(\Phi_1^*)} \int_0^{t^*} \Omega^{*\Phi_{2_*}-1}(t^* - \Omega^*)^{\Phi_1^*-1} |\mathcal{J}(\Omega^*, \mathcal{Q}(k^*))| dk^* \\
&\le \mathcal{Q}_0 + \frac{\Phi_{2_*}}{\Gamma(\Phi_1^*)} \int_0^{t^*} \Omega^{*\Phi_{2_*}-1}(t^* - \Omega^*)^{\Phi_1^*-1} \Theta^*(k^*)\mathbb{G}|\mathcal{J}(\mathcal{Q}(k^*))| d\Omega^* \\
&\le \mathcal{Q}_0 + \frac{\Phi_{2_*}\eta^*\eta^{\Phi_{2_*}+\Phi_{1_*}-1}\mathbb{B}(\Phi_{2_*}, \Phi_{1_*})}{\Gamma(\Phi_{1_*})} \Theta^*0^*\mathbf{A}(\|\mathcal{Q}\|_{\mathcal{H}^*}) \\
&\le \lambda + \zeta\Theta^*0^*\mathbf{A}(\nu).
\end{aligned}
\tag{23}
$$

Implying further that

$$\|\mathcal{W}\mathcal{Q}\| \le \lambda + \zeta\Theta^*0^*\mathbf{A}(\nu) < \infty. \tag{24}$$

We then obtain a complete continuous operator of $\mathcal{W}$ from $\mathcal{H}^*$. Let us now suppose some arbitrary values $t^*, t^{**} \in [0.T]$ such that $t^* \le t^{**}$ and also $\mathcal{Q} \in \mathcal{N}_\nu$ with the assumption that

$$\sup_{(t^*, \mathcal{Q}) \in \mathcal{A} \times \mathcal{N}_\nu} |\mathcal{J}(\Omega^*, \mathcal{Q}(t^*))| = \mathcal{J}^* < \infty.$$

It then suffices that

$$
\begin{aligned}
|\mathcal{W}(\mathcal{Q}(t^{**})) - \mathcal{W}(\mathcal{Q}(t^*))| &= |\frac{\Phi_{2_*}}{\Gamma(\Phi_1^*)} \int_0^{t^{**}} \Omega^{*\Phi_{2_*}-1}(t^{**} - \Omega^*)^{\Phi_1^*-1} |\mathcal{J}(\Omega^*, \mathcal{Q}(k^*))| dk^* \\
&\quad - \frac{\Phi_{2_*}}{\Gamma(\Phi_1^*)} \int_0^{t^*} \Omega^{*\Phi_{2_*}-1}(t^* - \Omega^*)^{\Phi_1^*-1} \Theta^*(k^*)\mathcal{J}|\mathcal{J}(\mathcal{Q}(k^*))| d\Omega^* \\
&\le \frac{\psi_{2_*}\mathcal{P}^*}{\Gamma(\psi_1^*)} |\int_0^{b^{**}} \Omega^{*\Phi_{2_*}-1}(t^{**} - \Omega^*)^{\Phi_1^*-1} dk^* - \int_0^{t^*} \Omega^{*\Phi_{2_*}-1}(t^* - \Omega^*)^{\Phi_1^*-1} dk^*| \\
&\le \frac{\Phi_{2_*}\mathbb{B}(\Phi_{2_*}, \Phi_1)\mathcal{J}^*}{\Gamma(\Phi_1^*)} [t^{**\Phi_{2_*}+\Phi_{1_*}-1} - t^{*\Phi_{2_*}+\Phi_{1_*}-1}] \\
&\le \frac{\Phi_{2_*}\Gamma(\Phi_{2_*})\mathcal{J}^*}{\Gamma(\Phi_1^* + \Phi_{1_*})} [(t^{**})^{\Phi_{2_*}+\Phi_{1_*}-1} - t^{*\Phi_{2_*}+\Phi_{1_*}-1}],
\end{aligned}
\tag{25}
$$

we therefore observe that $\mathcal{Q}$ is independent of t^{**} has a limit point in t^*, then the RHS of Eq. (25)

is asymptotic to 0. This leads to

$$\|\mathcal{W}(\mathcal{Q}(t^{**})) - \mathcal{W}(\mathcal{Q}(t^*))\|_{\mathcal{H}^*} \longrightarrow 0.$$

We then observe from the above that the function $\mathcal{W}$ is equi-continuous and we further show the compactness of $\mathcal{W}$ on $\mathcal{N}_\nu$ through means of the Arzela and Ascoli theorem. It is observed in furtherance that the assumptions given in Theorem 3 are explicitly valid on the function $\mathcal{V}$. This implies that either (a) or (b) is valid. From (M1), we formulate;

$$\mathcal{R} = \{\mathcal{Q} \in \mathcal{H}_* : \|\mathcal{Q}\|_{\mathcal{H}_*} < \mathcal{Z}\},$$

where we define the function $\mathcal{Z}$ to be positive through

$$\lambda + \zeta\Theta^*0^*\mathcal{B}(\mathcal{Z}).$$

Now by applying (M1) on Eq. (25) we derive the relation

$$\|\mathcal{W}\mathcal{Q}\|_{\mathcal{H}_*} \leq \lambda + \zeta\Theta^*0^*\mathbf{A}(\mathcal{Q}). \tag{26}$$

Now from the existence of the operator $\mathcal{Q} \in \beta\mathcal{R}$ and $\beta \in (0,1)$ in a manner that $\mathcal{Q} = \varrho\mathcal{W}(\mathcal{Q})$. Now by the given function $\mathcal{Q}$ in the domain β, then from Eq. (26), we have,

$$\mathcal{Z} = \|\mathcal{Q}\|_{\mathcal{H}^*} = \beta\|\mathcal{W}(\mathcal{Q})\|_{\mathcal{H}^*} < \lambda + \zeta\Theta^*0^*\mathbf{A}(\|\mathcal{Q}\|_{\mathcal{H}^*}) < \lambda + \zeta\Theta^*0^*\mathcal{Z}(\mathcal{R}) < \mathcal{R}.$$

From the above, we observe that we cannot validate it. This implies that (b) is invalid and the operator $\mathcal{W}$ has a solution or a fixed point in the function $\mathcal{R}$ from Theorem 3. Then, the Caputo fractal-fractional model has at least one solution.

Now we establish explicitly that the Caputo fractal-fractional model has only one solution. We begin by stating the lemma below;

Lemma 1 *Supposing that there exist the following functions:*
$(S, I, T, R, S^*, I^*, T^*, R^*) \in \mathcal{G} = C(\mathcal{N}, \mathcal{Y})$ and there is the norm
(N1): $\|S\| \leq \mathfrak{I}_1, \|I\| \leq \mathfrak{I}_2, \|T\| \leq \mathfrak{I}_3, \|R\| \leq \mathfrak{I}_4$ where $\mathfrak{I}_1, \mathfrak{I}_2, \mathfrak{I}_3, \mathfrak{I}_4$ are positive, and the given norms suffices the criteria of the least upper bound-norm regarding t^*. Now, further considering the case where, $\mathcal{J}_1, \mathcal{J}_2, \mathcal{J}_3, \mathcal{J}_4$ in view that equation the individual components in (11) meets the Lipschitz criterion of boundedness anytime there is $\mathcal{K}_1, \mathcal{K}_2, \mathcal{K}_3, \mathcal{K}_4 > 0$ where

$$\begin{aligned}\mathcal{K}_1 &= \alpha + \mu, \\ \mathcal{K}_2 &= (\alpha - \beta + \delta_1 + \mu), \\ \mathcal{K}_3 &= (\mu + \kappa + \sigma_2), \\ \mathcal{K}_4 &= \sigma_1 + \mu.\end{aligned}$$

Proof Given the first operator $\mathcal{P}_1$, for the dual functions, S, S^*, we compute;

$$\begin{aligned}\|\mathcal{J}_1(t^*, &S(t^*), I(t^*), T(t^*), R(t^*)) - \mathcal{J}_1(t_*, S^*(t^*), I^*(t^*), T^*(t^*), R^*(t^*))\| \\ &\leq \|\psi + \sigma_1 R(t) - \alpha_1 S(t)I(t) - \mu S(t)\| \leq -\alpha(S - S^*) - \mu(S - S^*) \\ &\leq \mathcal{K}_1\|S - S^*\|.\end{aligned}$$

We observe from the above that the function $\mathcal{J}_1$ about the compartment S for the constant $\mathcal{K}_1$ is positive and therefore bounded. Also, let us consider $\mathcal{J}_2$, for the dual functions, I, I^*, we obtain;

$$\|\mathcal{J}_1(t^*, S^*(t^*), I^*(t^*), T^*(t^*), R^*(t^*)) - \mathcal{J}_1(t_*, S^*(t^*), I^*(t^*), T^*(t^*), R^*(t^*))\|$$
$$\leq \|\alpha_1 S(t)I(t) + \kappa T(t) - \alpha_2 I(t)R(t) - (\beta + \delta_1 + \mu)I(t)\|$$
$$\leq [-\alpha - (\beta + \delta_1 + \mu)](I - I^*)$$
$$\leq -[\alpha - (\beta + \delta_1 + \mu)]\|I - I^*\|$$
$$\leq (\alpha - \beta + \delta_1 + \mu)\|I - I^*\|$$
$$\leq \mathcal{K}_2\|I - I^*\|.$$

We further observe that the function $\mathcal{J}_2$ about the compartment I for the constant $\mathcal{K}_2$ is positive and also bounded. Let us again consider $\mathcal{J}_3$, for the dual functions, T, T^*, we have;

$$\|\mathcal{J}_1(t^*, S(t^*), I(t^*), T(t^*), R(t^*)) - \mathcal{J}_1(t_*, S^*(t^*), I^*(t^*), T^*(t^*), R^*(t^*))\|$$
$$\leq \|\alpha_2 I(t)R(t)\beta I(t) - (\mu + \kappa + \sigma_2)T(t)\|$$
$$\leq -(\mu + \kappa + \sigma_2)(T - T^*)$$
$$\leq (\mu + \kappa + \sigma_2)\|T - T^*\|$$
$$\leq \mathcal{K}_3\|T - T^*\|.$$

In addition, we see again that the function $\mathcal{J}_3$ about the compartment T for the constant $\mathcal{K}_3$ is positive and therefore bounded. Let us finally consider $\mathcal{J}_4$, for the dual functions, R, R^*, we derive;

$$\|\mathcal{J}_1(t^*, S(t^*), I(t^*), T(t^*), R(t^*)) - \mathcal{J}_1(t_*, S^*(t^*), I^*(t^*), T^*(t^*), R^*(t^*))\|$$
$$\leq \|\sigma_2 T(t) - (\sigma_1 + \mu)R(t)\|$$
$$\leq -(\sigma_1 + \mu)(R - R^*)$$
$$\leq (\sigma_1 + \mu)\beta\|R - R^*\|$$
$$\leq (\sigma_1 + \mu)\|R - R^*\|$$
$$\leq \mathcal{K}_4\|R - R^*\|.$$

Finally, we observe that the function $\mathcal{J}_4$ about the state variable R for the constant $\mathcal{K}_4$ is positive and therefore bounded. This suffices that the constants $\mathcal{K}_1, \mathcal{K}_2, \mathcal{K}_3, \mathcal{K}_4$ meets the Lipscitz criterion for boundedness.

Let us finally state and prove the theorem below.

Theorem 5 *By assuming further that the condition (N1) is true, it is obvious that the Caputo fractal-fractional Ebola disease model admits only one solution whenever*

$$\circledast \mathcal{K}_\Omega < 1, \qquad \Omega \in \{1, 2, 3, 4\}, \tag{27}$$

recalling the definition of $\circledast$ in Eq. (22).

Proof By recalling and applying the concept of proof by contradiction, the study posits that the Caputo fractal-fractional Ebola model admits several solutions. We then commence the proof by assuming that there exists another solution to the Caputo fractal-fractional Ebola model, which is given as $(S^*(t^*), I^*(t^*), T^*(t^*), R^*(t^*))$ with the following initial values; (S_0, I_0, T_0, R_0) such that

Eq. (18) yields;

$$
\begin{aligned}
S^*(t^*) = S_0 + \frac{\Phi_{2*}}{\Gamma(\Phi_{1*})} \int_0^{\flat^*} & \Omega^{*\Phi_{2*}-1}(t^* - \Omega^*)^{\Phi_1^*-1} \\
& \times \mathcal{J}_1(\Omega^*, S^*(\Omega^*), I^*(\Omega^*), T^*(\Omega^*), R^*(\Omega^*))g^*\Omega^*, \\
I^*(t^*) = I_0 + \frac{\Phi_{2*}}{\Gamma(\Phi_{1*})} \int_0^{\flat^*} & \Omega^{*\Phi_{2*}-1}(t^* - \Omega^*)^{\Phi_1^*-1} \\
& \times \mathcal{J}_2(\Omega^*, S^*(\Omega^*), I^*(\Omega^*), T^*(\Omega^*), R^*(\Omega^*))g^*\Omega^*, \\
T^*(t^*) = T_0 + \frac{\Phi_{2*}}{\Gamma(\Phi_{1*})} \int_0^{\flat^*} & \Omega^{*\Phi_{2*}-1}(t^* - \Omega^*)^{\Phi_1^*-1} \\
& \times \mathcal{J}_3(\Omega^*, S^*(\Omega^*), I^*(\Omega^*), T^*(\Omega^*), R^*(\Omega^*))g^*\Omega^*, \\
R^*(t^*) = R_0 + \frac{\Phi_{2*}}{\Gamma(\Phi_{1*})} \int_0^{\flat^*} & \Omega^{*\Phi_{2*}-1}(t^* - \Omega^*)^{\Phi_1^*-1} \\
& \times \mathcal{J}_4(\Omega^*, S^*(\Omega^*), I^*(\Omega^*), T^*(\Omega^*), R^*(\Omega^*))g^*\Omega^*.
\end{aligned}
\tag{28}
$$

We then obtain the following results;

$$
\begin{aligned}
|S(t^*) - S^*(t^*)| \leq S_0 + \frac{\Phi_{2*}}{\Gamma(\Phi_{1*})} \int_0^{t^*} & \Omega^{*\Phi_{2*}-1}(t^* - \Omega^*)^{\Phi_1^*-1} \\
& \times |\mathcal{J}_1(\Omega^*, S(\Omega^*), I(\Omega^*), T(\Omega^*), R(\Omega^*)) \\
& - \mathcal{J}_1(\Omega^*, S(\Omega^*), I(\Omega^*), T(\Omega^*), R(\Omega^*))|g^*\Omega^* \\
\leq \frac{\Phi_{2*}}{\Gamma(\Phi_{1*})} \int_0^{t^*} & \Omega^{*\Phi_{2*}-1}(t^* - \Omega^*)^{\Phi_1^*-1} m_1 \|S - S^*\| g^*\Omega^* \\
\leq \circledast \mathcal{K}_1 \|S - S^*\|,
\end{aligned}
\tag{29}
$$

which in this case results in

$$
(1 - \circledast \mathcal{K}_1)\|S - S^*\| \leq 0.
$$

It is therefore obvious from Eq. (29) the inequality above will be true if $\|S - S^*\| = 0$ or S being the same as S^*.

Also considering the infected compartment, that is, $I(t)$, we obtain;

$$
\begin{aligned}
|I(t^*) - I^*(t^*)| \leq I_0 + \frac{\Phi_{2*}}{\Gamma(\Phi_{1*})} \int_0^{t^*} & \Omega^{*\Phi_{2*}-1}(t^* - \Omega^*)^{\Phi_1^*-1} \\
& \times |\mathcal{J}_2(\Omega^*, S(\Omega^*), I(\Omega^*), T(\Omega^*), R(\Omega^*)) \\
& - \mathcal{J}_2(\Omega^*, S(\Omega^*), I(\Omega^*), T(\Omega^*), R(\Omega^*))|g^*\Omega^* \\
\leq \frac{\Phi_{2*}}{\Gamma(\Phi_{1*})} \int_0^{t^*} & \Omega^{*\Phi_{2*}-1}(t^* - \Omega^*)^{\Phi_1^*-1} m_1 \|I - I^*\| g^*\Omega^* \\
\leq \circledast \mathcal{K}_2 \|I - I^*\|,
\end{aligned}
\tag{30}
$$

which in this case results in

$$
(1 - \circledast \mathcal{K}_2)\|V_1 - V_1^*\| \leq 0.
$$

It is then an obvious observation that from Eq. (30), the above inequality will be valid if $\|I - I^*\| = 0$ or I being the same as I^*.

Let us consider also the third compartment, that is, $T(t)$, we have;

$$
\begin{aligned}
|T(t^*) - T^*(t^*)| &\leq T_0 + \frac{\Phi_{2_*}}{\Gamma(\Phi_{1^*})} \int_0^{t^*} \Omega^{*\Phi_{2_*}-1}(t^* - \Omega^*)^{\Phi_1^*-1} \\
&\times |\mathcal{J}_3(\Omega^*, S(\Omega^*), I(\Omega^*), T(\Omega^*), R(\Omega^*)) \\
&- \mathcal{J}_3(\Omega^*, S(\Omega^*), I(\Omega^*), T(\Omega^*), R(\Omega^*))|g^*\Omega^* \\
&\leq \frac{\Phi_{2_*}}{\Gamma(\Phi_{1^*})} \int_0^{t^*} \Omega^{*\Phi_{2_*}-1}(t^* - \Omega^*)^{\Phi_1^*-1}m_1\|T - T^*\|g^*\Omega^* \\
&\leq \circledast\mathcal{K}_3\|T - T^*\|,
\end{aligned}
\tag{31}
$$

which also leads to

$$(1 - \circledast\mathcal{K}_3)\|T - T^*\| \leq 0.$$

We also see that from Eq. (31) the above inequality will be correct if $\|T - T^*\| = 0$ or T being the same as T^*.

Finally, considering the last state variable, that is, $R(t)$, we obtain;

$$
\begin{aligned}
|R(t^*) - R^*(t^*)| &\leq R_0 + \frac{\Phi_{2_*}}{\Gamma(\Phi_{1^*})} \int_0^{t^*} \Omega^{*\Phi_{2_*}-1}(t^* - \Omega^*)^{\Phi_1^*-1} \\
&\times |\mathcal{J}_4(\Omega^*, S(\Omega^*), I(\Omega^*), T(\Omega^*), R(\Omega^*)) \\
&- \mathcal{J}_4(\Omega^*, S(\Omega^*), I(\Omega^*), T(\Omega^*), R(\Omega^*))|g^*\Omega^* \\
&\leq \frac{\Phi_{2_*}}{\Gamma(\Phi_{1^*})} \int_0^{t^*} \Omega^{*\Phi_{2_*}-1}(t^* - \Omega^*)^{\Phi_1^*-1}m_1\|R - R^*\|g^*\Omega^* \\
&\leq \circledast\mathcal{K}_4\|R - R^*\|,
\end{aligned}
\tag{32}
$$

a similar result is obtained as

$$(1 - \circledast\mathcal{K}_4)\|R - R^*\| \leq 0.$$

It is therefore obvious from Eq. (32) the inequality above will be true if $\|R - R^*\| = 0$ or R being the same as R^*.

From the above results, it is implied that the current solution $(S^*(t^*), I^*(t^*), T^*(t^*), R^*(t^*))$ and the previous solution $(S(t^*), I(t^*), T(t^*), R(t^*))$ are the same. This suffices therefore that the Caputo fractal-fractional Ebola disease model admits a single solution. This ends the proof.

Hyers-Ulam and Hyers-Ulam-Rassias stability of the Caputo fractal-fractional Ebola model

This section is dedicated to the stability analysis of the model in Eq. (9). Stability analysis is carried out in this study to establish that the solutions of the model obtained are not absolutely dependent on the changes that may occur in the neighbourhood. This is essential as biological systems undergo changes sometimes and this may affect the nature of the solution obtained. The stability studies are therefore carried out to find out if a small change in the neighbourhood may exert the same small amount of change in the solution of the model. To conduct this study, we employ the Hyers-Ulam (HU) stability criterion [44] and its extended form referred to as

the Hyers-Ulam-Rassias stability (HUR) criterion [45]. Also, many models do not have exact solutions therefore resulting in mostly reliance on numerical solutions which also come from approximation algorithms. The HU and HUR stability criteria have shown enough strength in studying instabilities that may occur. This section therefore deals with applying the HU and HUR stability criteria to understand the stability patterns of the Caputo Ebola fractal-fractional model's solution.

Definition 4 *Let us suppose that the Caputo fractal-fractional Ebola model meets the HU stability criterion whenever there exist $D_{\mathcal{J}_i} > 0 \in \mathbb{R}$ for $i = 1, 2, 3, 4$ such that $\forall \wp > 0$ and also for every S^*, I^*, T^*, R^* in the set $\mathcal{S}^*$, then we have,*

$$
\begin{aligned}
|{}^{FFC}\mathcal{D}_{0,t^*}^{\Phi_1^*, \Phi_{2*}} S(t^*) - \mathcal{J}_1(S^*(t^*), I^*(t^*), T^*(t^*), R^*(t^*))| &< \wp_1, \\
|{}^{FFC}\mathcal{D}_{0,t^*}^{\Phi_1^*, \Phi_{2*}} I(t^*) - \mathcal{J}_2(S^*(t^*), I^*(t^*), T^*(t^*), R^*(t^*))| &< \wp_2, \\
|{}^{FFC}\mathcal{D}_{0,t^*}^{\Phi_1^*, \Phi_{2*}} T(t^*) - \mathcal{J}_3(S^*(t^*), I^*(t^*), T^*(t^*), R^*(t^*))| &< \wp_3, \\
|{}^{FFC}\mathcal{D}_{0,t^*}^{\Phi_1^*, \Phi_{2*}} R(t^*) - \mathcal{J}_4(S^*(t^*), I^*(t^*), T^*(t^*), R^*(t^*))| &< \wp_4,
\end{aligned}
\tag{33}
$$

and noting also that there exists $(S, I, T, R) \in \mathcal{S}^*$ then it is obvious that the Caputo fractal-fractional Ebola disease model satisfy

$$
\begin{aligned}
|S^*(t^*) - S(t^*)| &< D_{\mathcal{J}_1} \wp_1, \\
|I^*(t^*) - I(t^*)| &< D_{\mathcal{J}_2} \wp_2, \\
|T^*(t^*) - T(t^*)| &< D_{\mathcal{J}_3} \wp_3, \\
|R^*(t^*) - R(t^*)| &< D_{\mathcal{J}_4} \wp_4.
\end{aligned}
\tag{34}
$$

Remark 2 *We then suppose that $(S^*, I^*, T^*, R^*) \in \mathcal{G}^*$ is a solution to the Caputo fractal-fractional Ebola model whenever we have $\ell_1, \ell_2, \ell_3, \ell_4 \in \mathcal{C}([0, T], \mathbb{R})$ (based on (S^*, I^*, T^*, R^*) respectively) such that $\forall t^* \in (V, (\Omega)).|\ell_\Omega(t^*)| < \wp_\Omega$ for $\Omega = 1, 2, 3, 4$, given*

$$
\begin{aligned}
{}^{FFC}\mathcal{D}_{0,t^*}^{\Phi_1^*, \Phi_{2*}} S^*(t^*) &= \mathcal{J}_1(S^*(t^*), I^*(t^*), T^*(t^*), R^*(t^*))| + \wp_1(t^*), \\
{}^{FFC}\mathcal{D}_{0,t^*}^{\Phi_1^*, \Phi_{2*}} I^*(t^*) &= \mathcal{J}_2(S^*(t^*), I^*(t^*), T^*(t^*), R^*(t^*))| + \wp_2(t^*), \\
{}^{FFC}\mathcal{D}_{0,t^*}^{\Phi_1^*, \Phi_{2*}} T^*(t^*) &= \mathcal{J}_3(S^*(t^*), I^*(t^*), T^*(t^*), R^*(t^*))| + \wp_3(t^*), \\
{}^{FFC}\mathcal{D}_{0,t^*}^{\Phi_1^*, \Phi_{2*}} R^*(t^*) &= \mathcal{J}_4(S^*(t^*), I^*(t^*), T^*(t^*), R^*(t^*))| + \wp_4(t^*).
\end{aligned}
\tag{35}
$$

Definition 5 *We assume that the Caputo fractal-fractional Ebola model is HUR stable whenever we have a function Φ_i for $i = 1, 2, 3, 4$ for $D_{\mathcal{J}_i, \Phi_i} > 0 \in \mathbb{R}$ for $i = 1, 2, 3, 4$ such that for every $\wp_i > 0$ and also anytime $(S^*, I^*, T^*, R^*) \in \mathbb{S}^*$ satisfying*

$$
\begin{aligned}
|{}^{FFC}\mathcal{D}_{0,t^*}^{\Phi_1^*, \Phi_{2*}} S(t^*) - \mathcal{J}_1(S^*(t^*), I^*(t^*), T^*(t^*), R^*(t^*))| &< \wp_1 \Phi_1(t^*), \\
|{}^{FFC}\mathcal{D}_{0,t^*}^{\Phi_1^*, \Phi_{2*}} I(t^*) - \mathcal{J}_2(S^*(t^*), I^*(t^*), T^*(t^*), R^*(t^*))| &< \wp_2 \Phi_2(t^*), \\
|{}^{FFC}\mathcal{D}_{0,t^*}^{\Phi_1^*, \Phi_{2*}} T(t^*) - \mathcal{J}_3(S^*(t^*), I^*(t^*), T^*(t^*), R^*(t^*))| &< \wp_3 \Phi_3(t^*), \\
|{}^{FFC}\mathcal{D}_{0,t^*}^{\Phi_1^*, \Phi_{2*}} R(t^*) - \mathcal{J}_4(S^*(t^*), I^*(t^*), T^*(t^*), R^*(t^*))| &< \wp_4 \Phi_4(t^*),
\end{aligned}
\tag{36}
$$

this implies that $(S^*, I^*, T^*, R^*) \in \mathcal{U}^*$ satisfying the Caputo fractal-fractional Ebola model as given in

$$\begin{aligned}
|S^*(t^*) - S(t^*)| &< D_{\mathcal{J}_1 \Phi_1} \wp_1 \Phi_1(t^*), \\
|I^*(t^*) - I(t^*)| &< D_{\mathcal{J}_2 \Phi_2} \wp_2 \Phi_2(t^*), \\
|T^*(t^*) - T(t^*)| &< D_{\mathcal{J}_3 \Phi_3} \wp_3 \Phi_3(t^*), \\
|R^*(t^*) - R(t^*)| &< D_{\mathcal{J}_4 \Phi_4} \wp_4 \Phi_4(t^*).
\end{aligned} \tag{37}$$

Remark 3 *We then assume further that $(S^*, I^*, T^*, R^*) \in \mathcal{U}^*$ is a solution to the Caputo fractal-fractional Ebola model whenever we have $\ell_1, \ell_2, \ell_3, \ell_4 \in \mathcal{C}([0, T], \mathbb{R})$ (depending on (S^*, I^*, T^*, R^*) respectively) such that $\forall t^* \in (M, (\Omega)).|\ell_\Omega(t^*)| < \Phi_i \wp_\Omega$ for $\Omega = 1, 2, 3, 4$, given that*

$$\begin{aligned}
{}^{FFC}\mathcal{D}_{0,t^*}^{\Phi_1^*, \Phi_{2*}} S^*(t^*) &= \mathcal{J}_1(S^*(t^*), I^*(t^*), T^*(t^*), R^*(t^*))| + \wp_1(t^*), \\
{}^{FFC}\mathcal{D}_{0,t^*}^{\Phi_1^*, \Phi_{2*}} I^*(t^*) &= \mathcal{J}_2(S^*(t^*), I^*(t^*), T^*(t^*), R^*(t^*))| + \wp_2(t^*), \\
{}^{FFC}\mathcal{D}_{0,t^*}^{\Phi_1^*, \Phi_{2*}} T^*(t^*) &= \mathcal{J}_3(S^*(t^*), I^*(t^*), T^*(t^*), R^*(t^*))| + \wp_3(t^*), \\
{}^{FFC}\mathcal{D}_{0,t^*}^{\Phi_1^*, \Phi_{2*}} R^*(t^*) &= \mathcal{J}_4(S^*(t^*), I^*(t^*), T^*(t^*), R^*(t^*))| + \wp_4(t^*).
\end{aligned} \tag{38}$$

Theorem 6 *Let us suppose that the Caputo fractal-fractional Ebola model is HU stable and satisfies the condition that $U := [0, T]$ such that $\circledast \mathcal{K}_i$ for $i = 1, 2, 3, 4$, and $\circledast$ as defined in Eq. (22) and the axiom N1 is true.*

Proof By assuming that $\wp > 0$ and also we define $S^* \in \mathcal{G}$ given further that

$$|{}^{FFC}\mathcal{D}_{0,t}^{\Phi_1^*, \Phi_{2*}} S^*(t) - \mathcal{J}_1(S^*, I^*, T^*, R^*)| < \wp_1,$$

we then have ℓ_1 which is deduced from the condition in Remark 2, this then implies that;

$$\begin{aligned}
{}^{FFC}\mathcal{D}_{0,t}^{\Phi_1^*, \Phi_{2*}} S^*(t) &= \mathcal{J}_1(S^*, I^*, T^*, R^*) \\
&< \ell_1(t^*),
\end{aligned} \tag{39}$$

where $|\ell_1(t) \le \wp_1|$. This results in,

$$\begin{aligned}
S^*(t^*) = S_0 &+ \frac{\Phi_{2*}}{\Gamma(\Phi_1^*)} \int_0^{t^*} (t^* - \Omega^*)^{\Phi_1 - 1} \mathcal{J}_1(S^*(\Omega^*), I^*(\Omega^*), T^*(\Omega^*), R^*(\Omega^*)) d\Omega^* \\
&+ \frac{\Phi_{2*}}{\Gamma(\Phi_1^*)} \int_0^{t^{**}} (t^* - \Theta^*)^{\Phi_1^2 - 1} \wp_1(\Theta^*) d\Omega^*.
\end{aligned} \tag{40}$$

Now from Theorem 5, we let $S \in \mathcal{G}$ to be a unique solution of the measles disease model with Caputo fractal-fractional operators. The function $S(\flat^*)$ in the form

$$\begin{aligned}
S^*(t^*) = S_0 &+ \frac{\Phi_{2*}}{\Gamma(\Phi_1^*)} \int_0^{t^*} (t^* - \Omega^*)^{\Phi_1 - 1} \\
&\times \mathcal{J}_1(S^*(\Omega^*), I^*(\Omega^*), T^*(\Omega^*), R^*(\Omega^*)) d\Omega^*,
\end{aligned} \tag{41}$$

and this leads to,

$$
|S^*(t^*) - S(t^*)| \leq \frac{\Phi_{2_*}}{\Gamma(\Phi_1^*)} \int_0^{t^*} (t^* - \Omega^*)^{\Phi_1 - 1} |\wp_1(\Omega^*)| d\Omega^* + \frac{\Phi_{2_*}}{\Gamma(\Phi_1^*)} \int_0^{t^*} (t^* - \Omega^*)^{\Phi_1 - 1}
$$
$$
\times |\mathcal{J}_1(S^*(\Omega^*), I^*(\Omega^*), T^*(\Omega^*), R^*(\Omega^*)) d\Omega^* - \mathcal{A}_1(S(\Omega^*), I(\Omega^*), T(\Omega^*), R(\Omega^*)) d\Omega^*
$$
$$
\leq \circledast \wp_1 + \circledast \mathcal{K}_1 \|S^* - S\|.
$$

(42)

We then have;

$$
\|S^* - S\| \leq \frac{\circledast \wp_1}{1 - \circledast \mathcal{K}_1}.
$$

It is supposed that $D_{\mathcal{J}_1} = \frac{\circledast}{1 - \circledast \mathcal{K}_1}$, this then results in the norm $\|S^* - S\| \leq D_{\mathcal{J}_1, \wp_1}$. By following the same approach for the other state variables of the model, we obtain the norms below;

$$
\|I^* - I\| \leq D_{\mathcal{J}_2, \wp_2},
$$
$$
\|T^* - T\| \leq D_{\mathcal{J}_3, \wp_3},
$$
$$
\|R^* - R\| \leq D_{\mathcal{J}_4, \wp_4}.
$$

(43)

Since we have the results $D_{\mathcal{J}_i, \wp_i} = \frac{\circledast}{1 - \circledast \mathcal{K}_i}$ for $i = 2, 3, 4$, then the condition for stability is satisfied. Hence we posit that the Caputo fractal-fractional Ebola model meets the Hyers-Ulam stability criterion.

Theorem 7 *By assuming further that (N1) is valid, and we have some non-decreasing maps Φ_i contained in the set $C([0, T], \mathbb{R})$ for $i = 1, 2, 3, 4$ and also there exist some $\ell_{\Phi_i} > 0$ such that $\forall t^* \in U$, then we have*

$$
{}^{FFC}\mathcal{D}_{0,t}^{\Phi_1^*, \Phi_{2*}} \Phi_i(t^*) < \ell_{\Phi_i} \Phi_i(t^*), \qquad i = 1, 2, 3, 4.
$$

Whenever condition (N1) is satisfied, we say that the Caputo fractal-fractional Ebola model is Hyers-Ulam-Rassias stable.

Proof Given that $\wp > 0$ and also $S^* \in \mathcal{G}$, thius results in

$$
|{}^{FFC}\mathcal{D}_{0,t}^{\Phi_1^*, \Phi_{2*}} S^*(t^*) - \mathcal{J}_1 S^*(t^*), I^*(t^*), T^*(t^*), R^*(t^*)| < \wp_1 \Phi_i(t^*).
$$

Now assuming that there is $\ell_1(t^*)$ such that;

$$
{}^{FFC}\mathcal{D}_{0,t}^{\Phi_1^*, \Phi_{2*}} S^*(t^*) = \mathcal{J}_1 S^*(t^*), I^*(t^*), T^*(t^*), R^*(t^*) + \ell(t^*),
$$

noting that $|\ell_1(t^*) \leq \wp_1 \Phi_1(t^*)|$, leading to,

$$
S^*(t^*) = S_0 + \frac{\Phi_{2_*}}{\Gamma(\Phi_1^*)} \int_0^{t^*} (t^* - \Omega^*)^{\Phi_1 - 1} \mathcal{J}_1(S^*(\Omega^*), I^*(\Omega^*), T^*(\Omega^*), R^*(\Omega^*)) d\Omega^*
$$
$$
+ \frac{\Phi_{2_*}}{\Gamma(\Phi_1^*)} \int_0^{t^{**}} (t^* - \Omega^*)^{\Phi_1^2 - 1} \ell_1(\Omega^*) d\Omega^*.
$$

(44)

In addition, we recall from Theorem 5 and suppose that there exists a unique solution to the Caputo fractal-fractional Ebola model, relating to the state variable $S \in \mathcal{G}$. We then obtain the

function $S(t^*)$ in the form

$$
\begin{aligned}
S^*(t^*) = S_0 + \frac{\Phi_{2_*}}{\Gamma(\Phi_1^*)} \int_0^{t^*} (t^* - \Omega^*)^{\Phi_1 - 1} \\
\times \mathcal{J}_1(S^*(\Omega^*), I^*(\Omega^*), T^*(\Omega^*), R^*(\Omega^*)) d\Omega^*,
\end{aligned}
\tag{45}
$$

which then leads to,

$$
\begin{aligned}
|S^*(t^*) - S(t^*)| &\leq \frac{\Phi_{2_*}}{\Gamma(\Phi_1^*)} \int_0^{t^*} (t^* - \Omega^*)^{\Phi_1 - 1} |\wp_1(\Omega^*)| d\Omega^* \\
&\quad + \frac{\Phi_{2_*}}{\Gamma(\Phi_1^*)} \int_0^{t^*} (t^* - \Omega^*)^{\Phi_1 - 1} \\
&\quad \times |\mathcal{J}_1(S^*(\Omega^*), I^*(\Omega^*), T^*(\Omega^*), R^*(\Omega^*)) d\Omega^* \\
&\quad - \mathcal{A}_1(S(\Omega^*), I(\Omega^*), T(\Omega^*), R(\Omega^*)) d\Omega^* \\
&\leq \frac{\wp_1 \Phi_{2_*}}{\Gamma(\Phi_1^*)} \int_0^{t^*} (t^* - \Omega^*)^{\Phi_1 - 1} \Phi_1(t^*) + \circledast \mathcal{K}_1 \| S^* - S \| \\
&\leq \wp_1 \ell_{\Phi_1} \Phi_1(t^*) + \circledast \mathcal{K}_1 \| S^* - S \|.
\end{aligned}
\tag{46}
$$

It is observed that the state variable S is in the form;

$$
\| S^* - S \| \leq \frac{\wp_1 \ell_{\Phi_1} \Phi_1(t^*)}{1 - \circledast \mathcal{K}_1}.
$$

By concluding on this, from the above we define $D_{\mathcal{J}_1} = \frac{\ell_{\Phi_1}}{1 - \circledast \mathcal{K}_1}$, implying that the norm $\| S^* - S \| \leq \wp_1 D_{\mathcal{J}_1, \Phi_1} \Phi_1(t^*)$ is satisfied. Applying the same procedures we obtain the norms for the remaining state variables;

$$
\begin{aligned}
\| I^* - I \| &\leq \wp_2 D_{\mathcal{J}_2, \Phi_2} \Phi_2(t^*), \\
\| T^* - T \| &\leq \wp_3 D_{\mathcal{J}_3, \Phi_3} \Phi_3(t^*), \\
\| R^* - R \| &\leq \wp_4 D_{\mathcal{J}_4, \Phi_4} \Phi_4(t^*).
\end{aligned}
\tag{47}
$$

Finally, we recall that $D_{\mathcal{J}_i, \Phi_i} = \frac{\ell_{\Phi_i}}{1 - \circledast \mathcal{K}_i}$ for $i = 2, 3, 4$. It is then easy to conclude that the Caputo fractal-fractional Ebola model meets the Hyers-Ulam-Razzias stability criterion. This completes the proof.

6 Estimation of parameters

In this section, the estimation of parameters from real Ebola data is done for the model which is a crucial element of epidemiological modelling [46]. Future outcomes can be predicted using the model and advance our comprehension of the factors that influence the transmission of disease. Additionally, this method effectively finds the parameters that are very close to their actual data while producing the appropriate curve generated from actual data [47, 48]. In this study, the parameters of the model were obtained by applying the least-squares technique as used in literature, see for instance [49–52] and this yields estimated parameters that have the highest likelihood of being accurate, assuming certain crucial assumptions are met. Nonlinear least-squares analysis is a collection of numerical methods used to determine the best value for the parameters in a vector form based on experimental data. As a result, the model's solution is

accurately adjusted using the epidemic's real data. Eq. (48) provides the method of least-squares that we apply to investigate the model system. The method is to choose initial approximations and pre-calculated model parameters that offer a good fit or incorporate all of the data points by minimising the sum of the squared discrepancies between the model's solution and the observed data $\mathrm{II}(g, \tilde{m})$ [53, 54], such that:

$$\mathrm{II}(\tilde{m}) = \sum_{g=1}^{n} (\tilde{m}_g - \mathrm{II}(g, \tilde{m}))^2. \tag{48}$$

Data from the Ebola cases that took place in Uganda between September 10, 2022, and November 2, 2022, were utilised for the model fitting, and it is displayed in Table 1. As mentioned in [55, 56], the set of data was sourced from GitHub. In collaboration with the WHO Regional Office for Africa (WHO AFRO), the Ministry of Health in Uganda, and the ECDC surveillance provided the data. According to the data obtained from the Worldometer, the total population of Uganda was estimated to be 47,249,585 in 2022 [57]. Therefore, we chose this number to represent the entire population of Uganda, $N(0) = 47249585$. Initial populations of the state variables were selected as follows: $I(0) = 58, T(0) = 0, R(0) = 0$, and the initial number of susceptible humans is computed as $S(0) = N(0) - (I(0)) + T(0) + R(0)) = 47249527$. The incubation period, normally lasts between 2 and 21 days, by the WHO [58]. As per [2], 64.06 years was Uganda's life expectancy in 2022. Thus, the natural mortality rate is estimated to be $\mu = \frac{1}{64.06 \times 365}$. Hence, the rate at which people are recruited to join the susceptible class is computed as $\psi = \mu \times N = 2020$. Figure 1 displays the model fitting to the entire set of real data in Table 1. The data listed above and some educated guesses regarding the parameters were used to accomplish this. Table 2 displays the model parameters derived from the model calibration shown in Figure 1.

Table 1. Ebola disease human cases, from 10th October, 2022 to 2nd November, 2022

Day	Cases	Day	Cases
10/15/2022	58	10/25/2022	109
10/16/2022	60	10/26/2022	115
10/17/2022	60	10/27/2022	121
10/18/2022	61	10/28/2022	126
10/19/2022	64	10/29/2022	128
10/20/2022	65	10/30/2022	129
10/21/2022	71	10/31/2022	130
10/22/2022	75	11/01/2022	131
10/23/2022	90	11/02/2022	131
10/24/2022	95		

Table 2. Ebola model parameters

Parameter	Value/day	Source	Parameter	Value/day	Source
ψ	2020	Estimated	β	0.298548	Fitted
μ	$\frac{1}{64.06 \times 365}$	Estimated	σ_2	0.004703	Fitted
α_1	0.000019×10^{-3}	Fitted	δ_1	0.603885	Fitted
σ_1	0.002182	Fitted	α_2	0.023848	Fitted
κ	0.096099	Fitted			
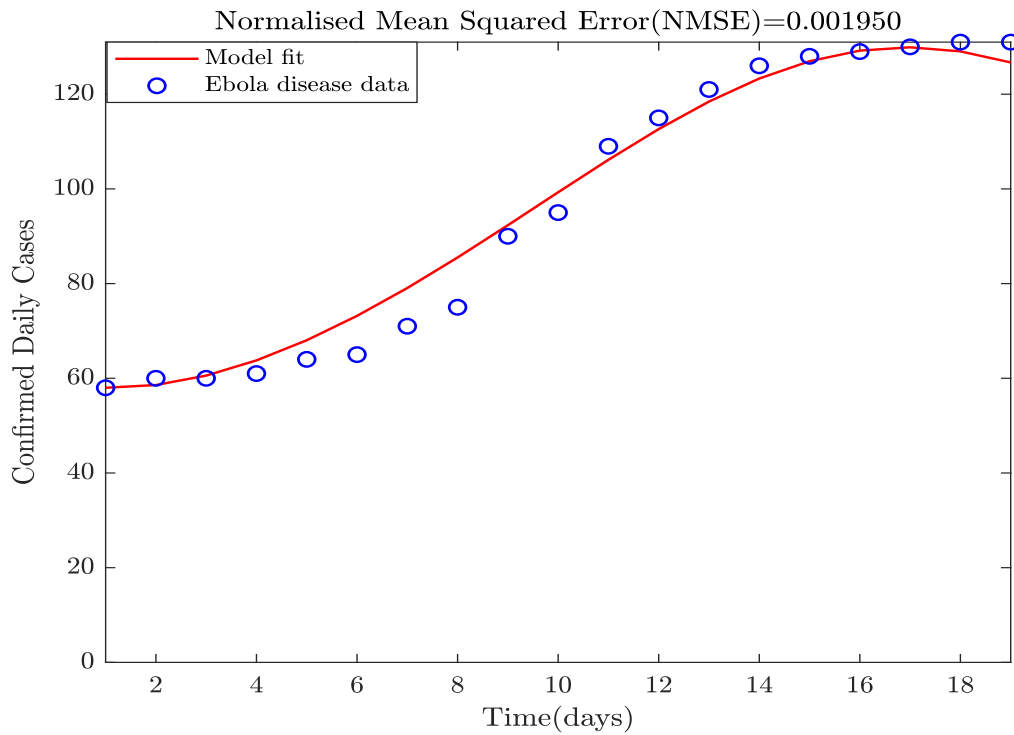
Figure 1. Comparison of the real data (blue dots) for the number of Ebola-infected individuals with the model under fractal-fractional Caputo derivative when $\Phi_1 = 0.80$ and $\Phi_2 = 0.86$ from 10th October, 2022 to 2nd November, 2022

7 Equilibrium points, stability of equilibrium points, and basic reproduction number

Disease-free equilibrium

The disease-free equilibrium denotes a situation where there is no disease in the population. It can be obtained in this model by setting S, I, T and R to zero in Eq. (1) and the resulting solution is given as

$$E_0 = \left(\frac{\psi}{\mu}, 0, 0, 0 \right). \tag{49}$$

The fundamental reproduction number

The reproduction number(R_0) is the mean number of subsequent infections introduced into a fully susceptible population by a single infected individual [1]. In epidemiology, R_0 is essential for comprehending how infectious diseases spread, directing public health initiatives, and assessing pathogen infectiousness for efficient disease control and prevention [28]. The R_0 value below 1 signifies the end of a disease outbreak, while an R_0 value above 1 suggests a potential epidemic. A reduction in reproduction numbers due to vaccination, social isolation, or quarantine measures indicates containment. Employing next-generation matrix approach, we derive the R_0 of the model (1) to be;

$$R_0 = \frac{1}{(\beta + \mu + \delta_1)} \left[\frac{\alpha_1 \psi}{\mu} + \frac{\beta k}{(\mu + k + \sigma_2)} \right]. \tag{50}$$

Analysis of disease-free equilibrium

In this subsection, we prove the local stability of E_0.

Theorem 8 *The disease-free equilibrium is locally asymptotically stable if $R_0 < 1$ and $(\beta + \mu + \delta_1) + (\mu + k + \sigma_2) > \alpha_1 \frac{\psi}{\mu}$ and unstable if $R_0 > 1$.*

Proof The corresponding Jacobian matrix of model (1) at E_0 is given by

$$J(E_0) = \begin{bmatrix} -\mu & -\alpha_1 \dfrac{\psi}{\mu} & 0 & \sigma_1 \\[2mm] 0 & \alpha_1 \dfrac{\psi}{\mu} - (\beta + \mu + \delta_1) & \kappa & 0 \\[2mm] 0 & \beta & -(\sigma_2 + \kappa + \mu) & 0 \\[2mm] 0 & 0 & \sigma_2 & -(\mu + \sigma_1) \end{bmatrix}. \tag{51}$$

It is obvious that Eq. (51) has two negative roots $\epsilon_1 = -\mu$ and $\epsilon_2 = -\mu - \sigma_1$. The rest of the roots would be obtained from the characteristic equation below

$$\epsilon^2 + [(\beta + \mu + \delta_1) + (\mu + \kappa + \sigma_2)] \epsilon + (\beta + \mu + \delta_1)(\mu + \kappa + \sigma_2)(1 - R_0). \tag{52}$$

From Eq. (51),

$$det(\epsilon_3 \epsilon_4) = (\beta + \mu + \delta_1)(\mu + \kappa + \sigma_2)(1 - R_0). \tag{53}$$

Also,

$$tr(\epsilon_3 + \epsilon_4) = \alpha_1 \frac{\psi}{\mu} - (\beta + \mu + \delta_1) - (\mu + \kappa + \sigma_2). \tag{54}$$

It is obvious that, since its trace is negative and its determinant is positive. $det(\epsilon_3 \epsilon_4) > 0$ if $R_0 < 1$. If

$$(\beta + \mu + \delta_1) + (\mu + \kappa + \sigma_2) > \alpha_1 \frac{\psi}{\mu}, \tag{55}$$

then $tr(\epsilon_3 + \epsilon_4) < 0$, implying that model (1) is asymptotically stable.

Existence of endemic equilibrium

Here, we examine the requirements for model (1)'s endemic equilibrium. The endemic equilibrium denoted by $E_1^{**} = (S^{**}, I^{**}, T^{**}, R^{**})$ is obtained by substituting the derivatives in the left-hand side of the model (1) and equate it to zero. We then solve the associated system of S^{**}, I^{**}, T^{**}, and R^{**}, we obtain

$$\begin{aligned} S^{**} &= \frac{\psi(\mu + \sigma_1)(\mu + k + \sigma_2) + \sigma_2 I^{**}(\psi \alpha_2 + \sigma_1 \beta)}{(\alpha_1 I^{**} + \mu)[(\mu + \sigma_1)(\mu + k + \sigma_2) - \alpha_2 \sigma_2 I^{**}]}, \\[2mm] T^{**} &= \frac{\beta(\mu + \sigma_1)I^{**}}{(\mu + \sigma_1)(\mu + k + \sigma_2) - \alpha_2 \sigma_2 I^{**}}, \\[2mm] R^{**} &= \frac{\beta \alpha_2 \sigma_2 I^{**}}{(\mu + \sigma_1)(\mu + k + \sigma_2) - \alpha_2 \sigma_2 I^{**}}. \end{aligned} \tag{56}$$

The endemic equilibrium (56) satisfies

$$P(I^{**}) = I^{**}(Q_1 I^{**})^2 + Q_2 I^{**} + Q_3) = 0, \tag{57}$$

where

$$Q_1 = \alpha_1 \alpha_2 \sigma_2 (\mu + \delta_1),$$
$$Q_2 = \alpha_2 \sigma_2 [\psi \alpha_1 + \mu(\mu + \delta_1)] + \alpha_1 \eta \sigma_2 + \alpha_1 (\eta + \mu)[k\beta - (k + \mu + \sigma_2)(\beta + \mu + \delta_1)],$$
$$Q_3 = (k + \mu + \sigma_2)(\beta + \mu + \delta_1)(\eta + \mu)(R_0 - 1).$$

The root $I^{**} = 0$ of Eq. (57) corresponds to disease-free equilibrium. Thus, we regard the quadratic equation

$$P(I^{**}) = Q_1 (I^{**})^2 + Q_2 I^{**} + Q_3 = 0, \tag{58}$$

in determining the existence of endemic equilibrium. It should be noted that the positive root of the equation provides the endemic equilibrium (56).

One can easily see that $Q_1 > 0$ whether $R_0 > 1$ or not. If $R_0 > 1$, $Q_3 > 0$ and if $Q_2 < 0$ when $R_0 > 1$, then the graph of the polynomial (58) indicates that model (1) has one endemic equilibrium. If $R_0 < 1$, and $Q_3 < 0$. Then model (1) has no endemic equilibrium. If $R_0 = 1$, $Q_2 > 0$ and $Q_3 = 0$, then Eq. (58) has no positive root. In conclusion, we arrive at the results below.

Theorem 9 *The model* (1) *has a unique endemic equilibrium if $Q_2 < 0$ and $R_0 > 1$, and no endemic equilibrium when $R_0 \leq 1$.*

Local stability of endemic equilibrium and bifurcation analysis

We examine the possibility of bifurcation and discuss the local stability of endemic equilibrium. The bifurcation phenomenon is established in this section by using the centre manifold theory as explained in Theorem 4.1 by both Carlos Castillo-Chavez et al. [59] and Buonomo et al. [60] respectively as follows:

We consider the transmission rate of Ebola α_1 as the bifurcation parameter so that $R_0 = 1$ if and only if

$$\alpha_1 = \alpha_1^* = \frac{\mu(\beta + \mu + \delta_1)(\mu + k + \sigma_2) - \beta k \mu}{\psi(\mu + k + \sigma_2)}.$$

Introducing $S = x_1$, $I = x_2$, $T = x_3$, and $R = x_4$, model (1) becomes

$$\begin{aligned}
f_1 &= x_1' = \psi + \sigma_1 x_4 - \alpha_1 x_1 x_2 - \mu x_1, \\
f_2 &= x_2' = \alpha_1 x_1 x_2 + k x_3 - \alpha_2 x_2 x_4 - (\beta + \mu + \delta_1) x_2, \\
f_3 &= x_3' = \alpha_2 x_2 x_4 + \beta x_2 - (\mu + k + \sigma_2) x_3, \\
f_4 &= x_4' = \phi x_3 - (\mu + \sigma_1) x_4.
\end{aligned} \tag{59}$$

We know that the Ebola-free equilibrium is $\left[x_1^* = \dfrac{\psi}{\mu}, x_2^* = 0, x_3^* = 0, x_4^* = 0\right]$. We linearised the matrix of the model (59) around the disease-free equilibrium when $\alpha_1 = \alpha_1^*$ and obtained

$$
J(E_1^0) = \begin{bmatrix}
-\mu & -\alpha_1\dfrac{\psi}{\mu} & 0 & \sigma_1 \\
0 & \alpha_1\dfrac{\psi}{\mu} - (\beta + \mu + \delta_1) & \kappa & 0 \\
0 & \beta & -(\sigma_2 + \kappa + \mu) & 0 \\
0 & 0 & \sigma_2 & -(\mu + \sigma_1)
\end{bmatrix}.
\tag{60}
$$

The matrix $J(E_1^0)$ possesses a simple eigenvalue, with other eigenvalues endowed with negative real parts. Therefore, the centre manifold theorem as performed in [2] can be applied. We therefore need to derive the values of a and b. We begin this by calculating the right and left eigenvalues of $J(E_1^0)$ denoted by

$$
W = [w_1, w_2, w_3, w_4]^T \quad \text{and} \quad V = [v_1, v_2, v_3, v_4], \quad \text{respectively.}
$$

We obtain

$$
w_1 = -\dfrac{\psi\alpha_1^*(\mu + k + \sigma_2)(\mu + \sigma_1) + \sigma_2\sigma_1\beta\mu}{\mu^2\beta\sigma_2}, \quad w_2 = \dfrac{(\mu + k + \sigma_2)(\mu + \sigma_1)}{\beta\sigma_2}, \quad w_3 = \dfrac{(\mu + \eta)}{\sigma_2},
$$

$$
w_4 = 1,
$$

and

$$
v_1 = 0, \quad v_2 = \dfrac{(\mu + k + \sigma_2)}{k}, \quad v_3 = 1, \quad \text{and} \quad v_4 = 0.
$$

Next, we compute the values of a and b. From model (59), all the associated partial derivatives of $F = (f_1, f_2, f_3, f_4)^T$ in (59) are zero at the Ebola-free equilibrium (DFE) except the following:

$$
\dfrac{\partial^2 f_1}{\partial x_1 \partial x_2} = \dfrac{\partial f_1}{\partial x_2 \partial x_1} = -\alpha_1^*, \quad \dfrac{\partial^2 f_2}{\partial x_1 \partial x_2} = \dfrac{\partial^2 f_2}{\partial x_2 \partial x_1} = \alpha_1^*, \quad \dfrac{\partial^2 f_2}{\partial x_2 \partial x_4} = \dfrac{\partial^2 f_2}{\partial x_4 \partial x_2} = -\alpha_2,
$$

$$
\dfrac{\partial^2 f_3}{\partial x_2 \partial x_4} = \dfrac{\partial^2 f_3}{\partial x_4 \partial x_2} = \alpha_2, \quad \dfrac{\partial^2 f_2}{\partial x_2 \partial \alpha_1^*} = \alpha_2, \quad \dfrac{\partial^2 f_2}{\partial x_3 \partial \alpha_1^*} = \dfrac{\psi}{\mu}.
$$

Substituting the above equations into a and b in

$$
a = \sum_{k,i,j=1}^{n} v_k w_i w_j \dfrac{\partial^2 f_k}{\partial x_i \partial x_j}(0,0),
$$

$$
b = \sum_{k,i=1}^{n} v_k w_i \dfrac{\partial^3 f_k}{\partial x_i \partial \phi}(0,0),
$$

it follows that

$$a = 2v_2 w_1 w_2 \frac{\partial^2 f_2}{\partial x_1 \partial x_2} + 2v_2 w_2 w_4 \frac{\partial^2 f_2}{\partial x_2 \partial x_4} + 2v_3 w_2 w_4 \frac{\partial^2 f_3}{\partial x_2 \partial x_4}$$

$$= 2v_2 w_1 w_2 \alpha_1^* - 2v_2 w_2 w_4 \alpha_2 + 2v_3 w_2 w_4 \alpha_2$$

$$= \frac{2(\mu + k + \sigma_2)^2 (\mu + \sigma_1)}{k \beta^2 \mu^2 \sigma_2^2} \left[\frac{\alpha_2}{(\mu + k + \sigma_2)} - \left(\psi \alpha_1^{*2} (\mu + k + \sigma_2)(\mu + \sigma_1) + \beta \mu (\alpha_2 \mu + \sigma_2 \sigma_1) \right) \right] > 0,$$

$$b = v_2 w_2 \frac{\partial^2 f_2}{\partial x_2 \partial \alpha_1^*} + v_3 w_3 \frac{\partial^2 f_2}{\partial x_3 \partial \alpha_1^*}$$

$$= \frac{\psi (k + \sigma_2 + \mu)^2 (\mu + \sigma_1)}{\beta \mu k \sigma_2} > 0.$$

Here, it is obvious that the coefficient $b > 0$. It follows from the results given in [61], that model (1) undergoes backward bifurcation whenever $a > 0$, that is $\frac{\alpha_2}{(\mu + k + \sigma_2)} > \left(\psi \alpha_1^{*2} (\mu + k + \sigma_2)(\mu + \sigma_1) + \beta \mu (\alpha_2 \mu + $ and would be a forward bifurcation whenever $a < 0$, that is $\frac{\alpha_2}{(\mu + k + \sigma_2)} < \left(\psi \alpha_1^{*2} (\mu + k + \sigma_2)(\mu + \sigma_1) + \beta \mu (\alpha_2 \mu + \sigma_2 \sigma_1) \right)$. The endemic equilibrium, which exists whenever $R_0 > 1$, is locally asymptotically stable whenever $R_0 > 1$ and $\alpha_1^* < \alpha_1$ with α_1 close to α_1^*.

Theorem 10 *The unique endemic equilibrium of model (59) is locally asymptotically stable when $R_0 > 1$.*

8 Sensitivity analysis of R_0

In this subsection, we conduct a sensitivity analysis of some key parameters in support of the graphs in Figure 6. The significance of conducting the sensitivity analysis is to identify parameters influencing the R_0. It is a useful tool for determining essential parameters to be considered while developing intervention strategies [2, 62, 63]. The forward normalised sensitivity index of R_0 is employed in this section. It is therefore defined as:

$$\chi_\ell^{R_0} = \frac{\partial R_0}{\partial \ell} \times \frac{\ell}{R_0}, \tag{61}$$

where ℓ denotes the parameters in the R_0. The resulting sensitivity indices utilising Eq. (4) and the parameter values in Table 2 are given in Table 3 below.

Table 3. Sensitivity analysis of R_0 to parameters for the Ebola model

Number	Parameter	Index
1	α_1	$+0.99968$
2	ψ	$+0.99968$
3	κ	$+1.49150 \times 10^{-5}$
4	μ	-0.99973
5	β	-0.33049
6	δ_1	-0.66914
7	σ_2	-1.47801×10^{-5}

Parameters with negative sensitivity indices lower R_0 value as the values assigned to them are increased. Parameters with positive indices increase R_0 value as the values assigned to the

(a) 3D plot of κ and σ_2 on R_0 **(b)** Contour plot
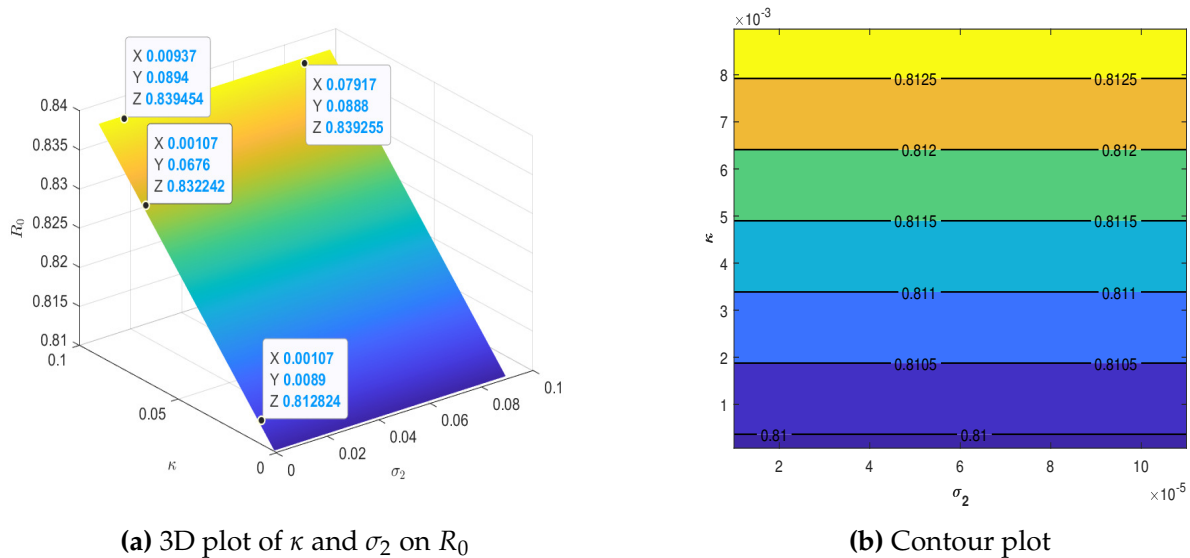
Figure 2. The effect of κ and σ_2 on R_0

parameters are increased. It can be seen from Table 3 that α_1, κ and ψ are positive. Therefore, increasing their values increases the value of R_0. For instance, increasing α_1 by 10% raises or reduces the R_0 value by 9.9968%. Figure 2 indicates the 3D and contour plots in support of the impact of relapse rate, κ and the recovery rate, σ_2 on R_0. It can be seen in Figure 2a and Figure 2b that the value of R_0 increases as the values of κ increase. Also, the R_0 value decreases as the value of σ_2 increases. This implies that Ebola transmission can be reduced if the values of κ are reduced while increasing the value of σ_2 so that the value of R_0 would be less than unity. This can be achieved by educating the susceptible to ensure personal protection against Ebola, disinfecting the environment of the infectious and Ebola-related death victims, and advising the infectious individuals to visit health centres for treatment and vaccination of susceptible individuals. Also, $\beta, \delta_1, \sigma_2,$ and μ have negative values. Therefore, an increase in any of them decreases the R_0. For instance, raising or lowering β by 10% raises or lowers the R_0 value by 3.3049%. This implies that if infectious people are advised to visit treatment centres Ebola infection decreases. Moreover, the rate of recovery of the infectious populace has been dominant. Thus, a reduction in R_0 to less than one will be possible if infected persons recover early from Ebola. However, the natural mortality rate, the disease-related death rate, and the recruitment rate cannot be used as control measures to eradicate the transmission of disease in our communities.

9 Numerical trajectories and discussion of results

In this subsection, the numerical results and the discussion of the outcomes of the analysis that was conducted in this study are presented. Based on the fractal-fractional Caputo, our model of the Ebola outbreak in Uganda may be numerically examined and utilised to predict the disease's trajectory. We used Newton's polynomial numerical scheme to carry out extensive numerical simulations, taking into consideration the estimated parameter values provided in Table 2. The numerical simulations were carried out using these initial state variable values: $S(0) = 47249527$, $I(0) = 58$, $T(0) = 0$, $R(0) = 0$, and the parameter values given in Table 2. Numerous simulations were conducted to assess the influence of the parameters on the Ebola virus disease state variables. Additionally, we performed sensitivity analyses on some of the key parameters to see how they affect the possibility of Ebola disease transmission.

The graphical results for our model's compartments, $S, I, T,$ and R, utilising different fractal-fractional order values are presented in Figure 3, Figure 4, and Figure 5 accordingly. It is observed

that all the state variables' trajectories show a consistent pattern of convergence toward the precise endemic equilibrium point. This portrays the real dynamics of the Ebola virus disease outbreak. First, we show the numerical solution for both the integer order and the fractal-fractal Caputo orders of model (2) in Figure 3. It is obvious from Figure 3a, Figure 3b, Figure 3c and Figure 3d that integer model with $\Phi_1 = \Phi_2 = 1$ recorded a lower count of susceptible whiles infectious, treatment and recovery classes recorded a higher count as compared to the fractal-fractional order models. The integer order raises the impact of Ebola. An interesting result was observed in Figure 3b. The number of individuals infected with the Ebola virus increases more quickly as the fractional values get closer to unity, but after 18 days, it begins to decline sharply. The disease's trajectory seems to record a moderate growing pace, we record greater sensitivity to it at $\Phi_1 = \Phi_2 = 1$. A similar result was obtained in Figure 4b and Figure 5b.

The simulation results in Figure 4 depict the impact of keeping the fractal dimension constant at $\Phi_1 = 1$ while varying the fractional order value. It was observed in Figure 4a, Figure 4b, Figure 4c, and Figure 4d that, individuals in the susceptible class increase as fractional order values decrease. Also, individuals in the infectious, treatment, and recovery classes reduce as the fractional value reduces. As shown in Figure 5a, Figure 5b, Figure 5c, and Figure 5d, increasing the fractal dimension for a constant fractional order value produces dynamics that are similar to those obtained by keeping the fractal dimension constant at $\Phi_1 = 1$ and varying the fractional order. The findings underscore the significance of employing fractal-fractional models modelling infectious diseases. Hidden patterns and structures in the natural phenomena of Ebola transmission have been discovered by the application of fractal-fractional Caputo derivatives. Additionally, we analysed the contribution of some key parameters to the Ebola transmission and presented the results in Figure 6a, Figure 6b, Figure 6c and Figure 6d. We observed that, as the values of transmission rate outside the treatment centres, α_1, and the relapse rate, κ increase, the number of Ebola infectious individuals increases as indicated in Figure 6a, and Figure 6d respectively. This implies that α_1, and κ significantly contribute to the endemic status of the disease by increasing the value of the reproduction ratio. They are among the essential components that need to be considered while developing intervention strategies to curb the Ebola outbreak. We suggest that the provision of an immune booster vaccination after treatment could offer active, long-term protection, lower relapse rates, and prevent fatal outcomes. Furthermore, implementing control measures like quarantine, isolation, and disinfecting the environment in Ebola-affected communities could potentially help many individuals recover from the disease. Moreover, we considered the transmission rate at treatment centres, α_2, and the rate of transfer from the treated class to the infected class, β. We observed from Figure 6c and Figure 6b that recovery increases at treatment centres as the transmission rate within treatment centres, α_2 decreases in value. Also, as the value of β increases, the rate of Ebola infection declines, as depicted in Figure 6b. This implies if many infectious individuals are advised to visit treatment centres, Ebola transmission reduced, in communities. This also implies that transmission of Ebola disease could be controlled if proper measures are put in place at treatment centres. For instance, the implementation of clinical daily surveillance or prophylaxis after exposure (PEP) with favipiravir, health care worker training, and the provision of personal protective equipment (PPE) items may all contribute to the reduction of infection rates within Ebola treatment centres. Again, Figure 7 indicates the effects of σ_2 on the R_0. It is obvious that as the value of σ_2 increases the number of Ebola infectious individuals decreases. Hence reduction in its value increases recovery of the disease. This suggests that if the transmission rate is lowered, the number of subsequent infections in the community can be decreased and the relapse rate of Ebola is reduced. These can be achieved through personal protection against the disease, vaccination, and treatment, and disinfecting the surroundings of the deceased Ebola victims. Finally, it is obvious that the fractional model is essential to comprehend the vital factors

and attain accuracy and consistency. Its memory effects are demonstrated through graphs, unlike the integer-order models. According to the World Health Organisation (WHO), the Ebola virus disease is severe and recorded a mortality rate of up to 90% in humans. Notwithstanding this, it further reports that by carrying out effective treatment strategies, the mortality rate has decreased drastically from 90% to 25% in current epidemics. This report is in line with the results from our study since when proper precautions are put in place at the treatment centres we observed an increase in the recovery compartment which implies a decline in the disease-induced mortality rate.
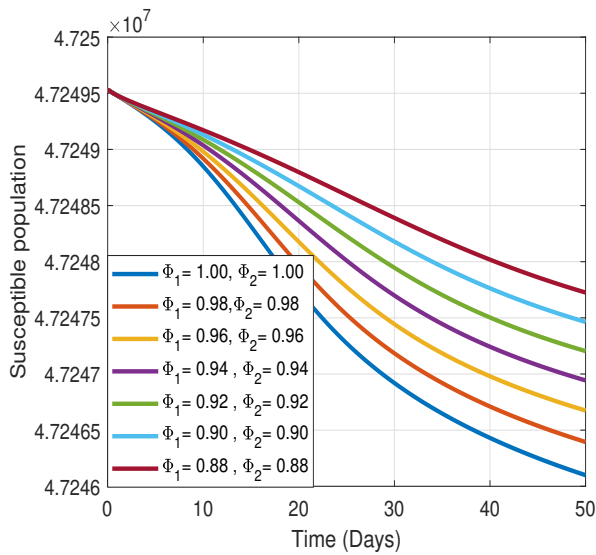
(a) Effect of Fractal-Fractional order on the susceptible class, $S(t)$
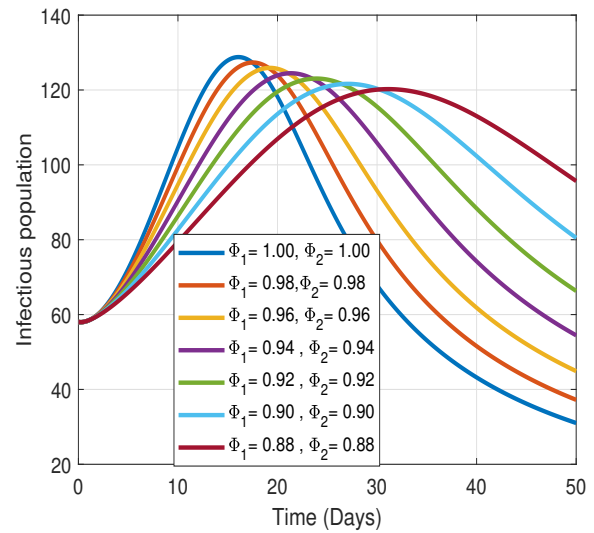
(b) Effect of Fractal-Fractional order on the infectious class, $I(t)$
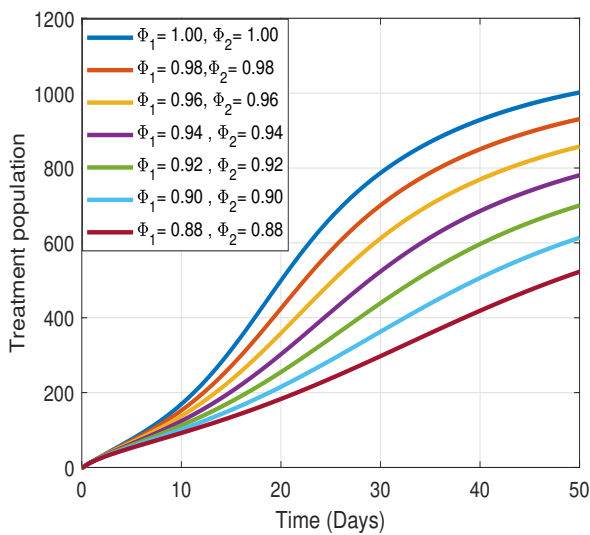
(c) Effect of Fractal-Fractional order on the treatment class, $T(t)$
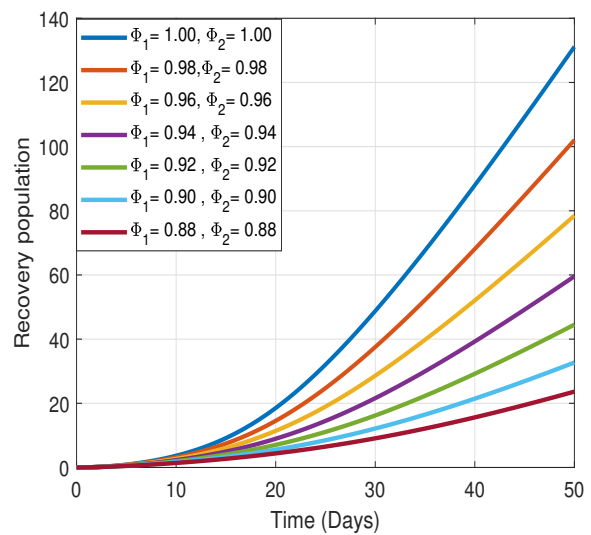
(d) Effect of Fractal-Fractional order on the recovery class, $R(t)$

Figure 3. Effect of Fractal-Fractional order on the $S(t), I(t), T(t)$, and $R(t)$ respectively. Considering $\Phi_1 = \Phi_2 = 1, 0.98, 0.96, 0.94, 0.92, 0.90, 0.88$
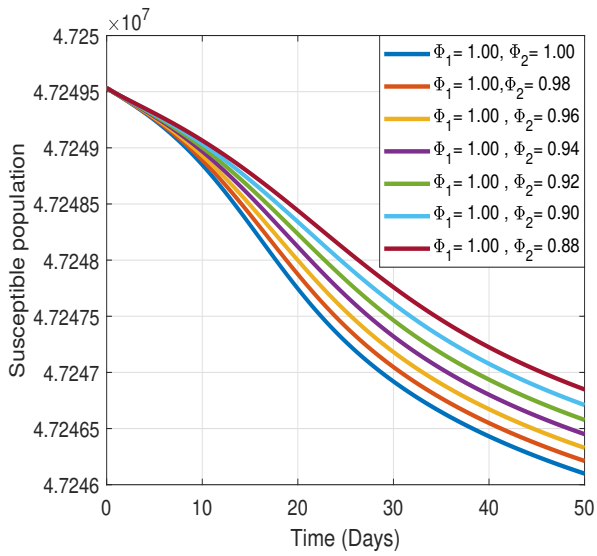
(a) Effect of Fractional order on the susceptible class, $S(t)$
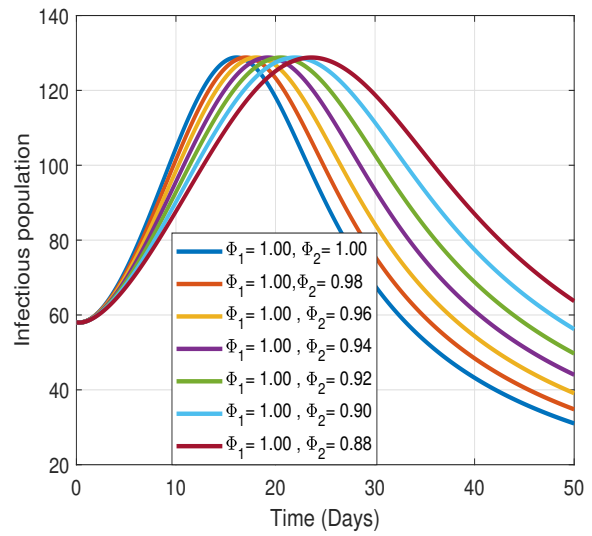
(b) Effect of Fractional order on the infectious class, $I(t)$
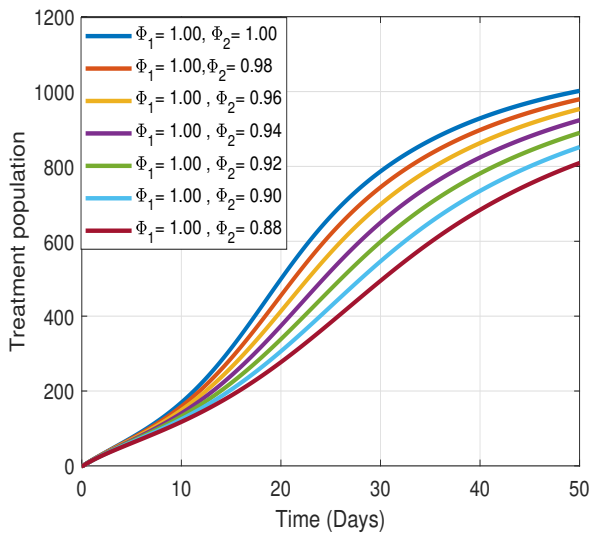
(c) Effect of Fractional order on the treatment class, $T(t)$
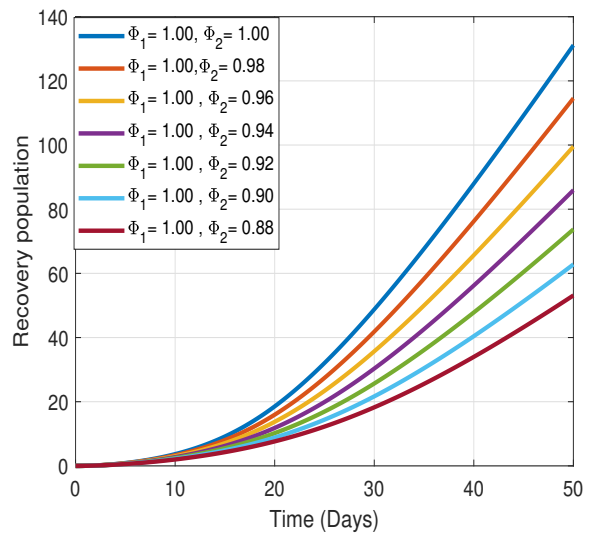
**(d)** Effect of fractional order on the recovery class, $R(t)$

Figure 4. Effect of fractional order on the $S(t), I(t), T(t)$, and $R(t)$ respectively. Considering $\Phi_1 = 1$ and $\Phi_2 = 1, 0.98, 0.96, 0.94, 0.92, 0.90, 0.88$
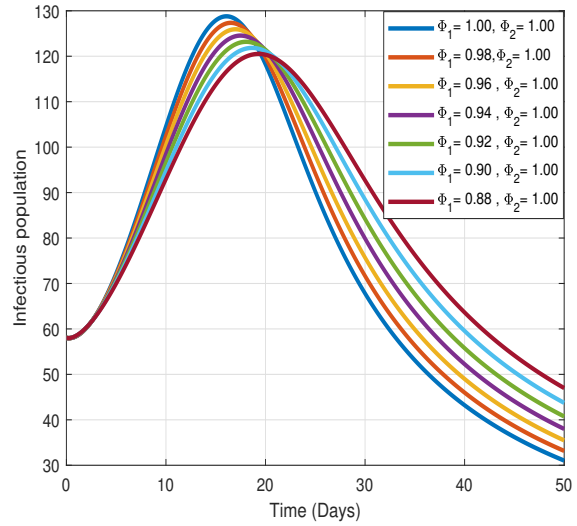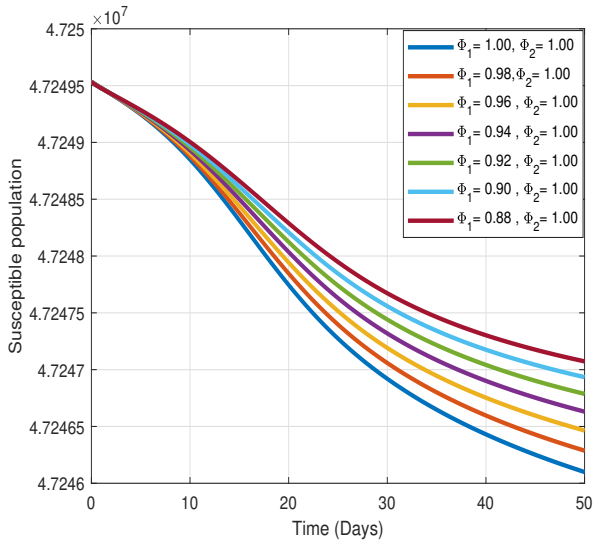
(a) Effect of Fractal order on the susceptible class, $S(t)$ **(b)** Effect of Fractal order on the infectious class, $I(t)$
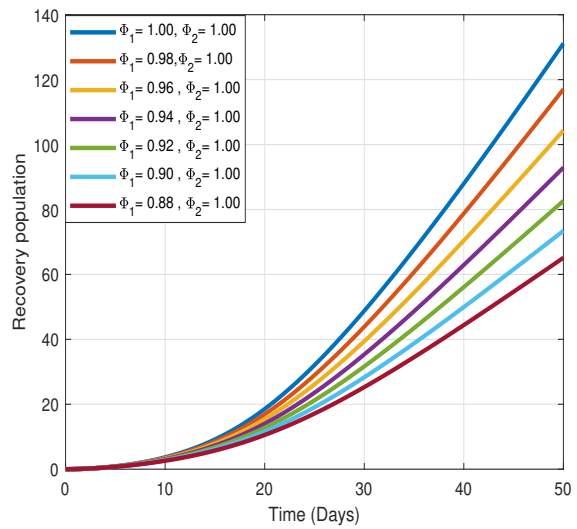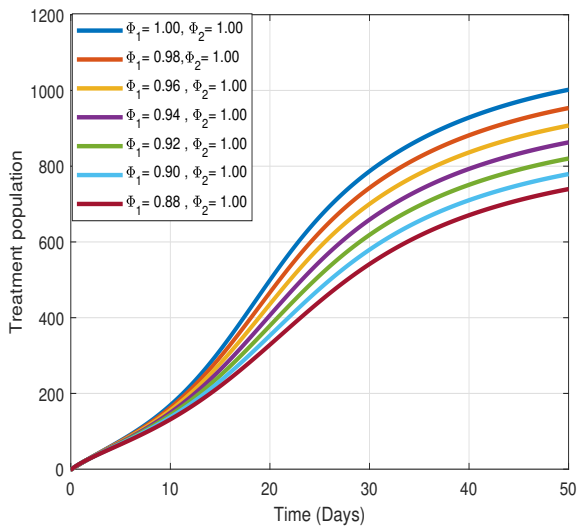
(c) Effect of Fractal order on the treatment class, $T(t)$ **(d)** Effect of Fractal order on the recovery class, $R(t)$

Figure 5.   Effect of Fractal order on the $S(t), I(t), T(t)$, and $R(t)$ respectively.   Considering $\Phi_1 = 1, 0.98, 0.96, 0.94, 0.92, 0.90, 0.88$ and $\Phi_2 = 1$
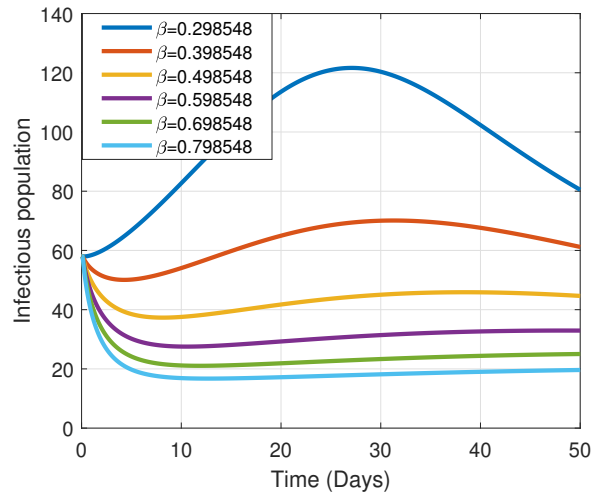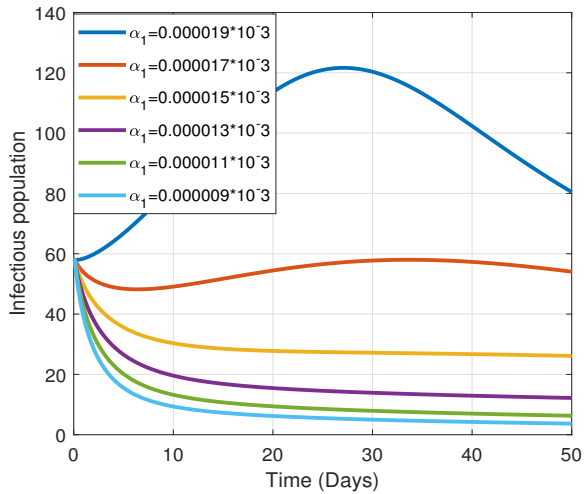
(a) Effect of α_1 on the infectious class, I(t) at $\Phi_1 = \Phi_2 = 0.90$

(b) Effect of β on the,infectious class, I(t) at $\Phi_1 = \Phi_2 = 0.90$
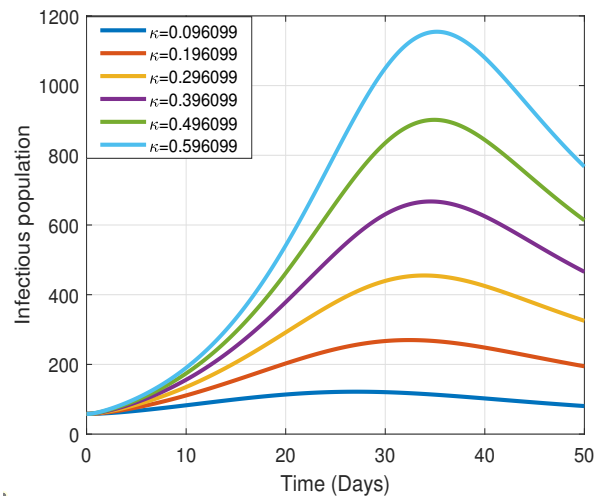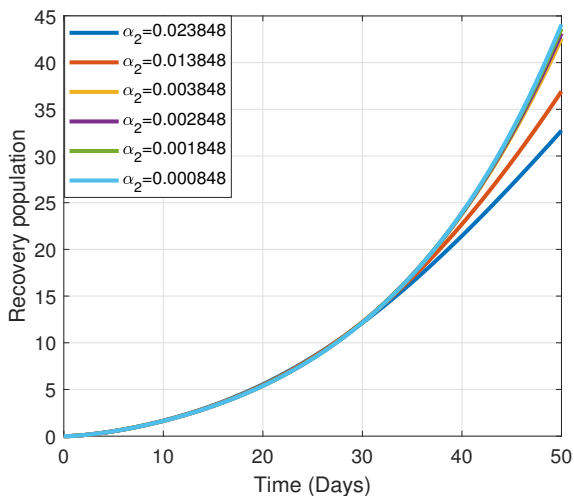
(c) Effect of α_2 on the recovery class, R(t) at $\Phi_1 = \Phi_2 = 0.90$

(d) Effect of κ on the infectious class, I(t) at $\Phi_1 = \Phi_2 = 0.90$

Figure 6. Effect of α_1, β, κ on the infectious class, I(t) and α_2 on the recovery class, R(t) at $\Phi_1 = \Phi_2 = 0.90$
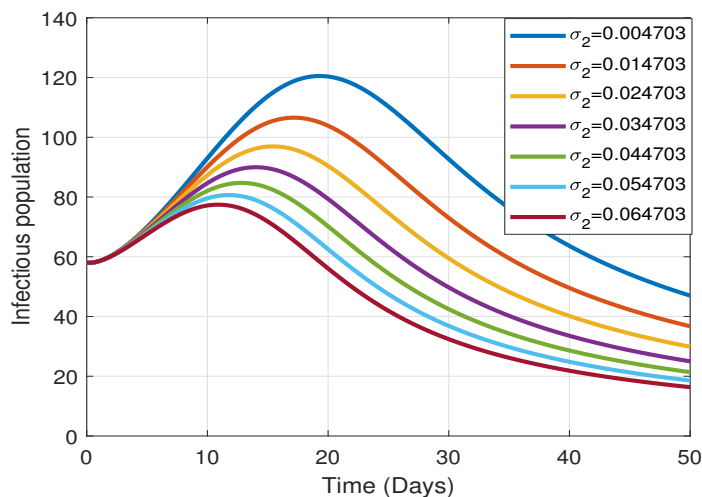
Figure 7. Effect of σ_2 on the infectious class, I(t) at $\Phi_1 = \Phi_2 = 0.90$

10 Conclusion

In this paper, the dynamics of the Ebola virus disease are investigated with a keen focus on the transmission of the Ebola virus disease at the treatment centres and also how the virus persists in the immunological sites of the treated patient which mostly results in the relapse of the disease. These dynamics of the Ebola virus disease are essential and contribute massively to the spread of the disease in the population. Therefore a Caputo fractal-fractional Ebola model was formulated to study how to control the disease in the population. The fractional operators were employed due to their ability to capture the memory effect exhibited by the Ebola virus disease. Through the fixed point theory, it was established that the Caputo fractal-fractional Ebola model possesses a unique solution. The study further applied the HU and HUR stability criteria to establish that the model was stable. In the studies, all parameters were fitted to real data from Uganda making the model's parameter values more reliable. It was observed from the sensitivity analysis that parameters like α_1, ψ and κ have a direct relationship with the spread of the disease whereas parameters like μ, β, δ_1 and σ_2 are inversely related to the fundamental reproductive number. From the numerical simulations, it was discovered that the hidden patterns or dynamics of the Ebola virus disease are well captured using fractional operators. It was observed that the transmission rate outside the treatment centres and relapse rate resulted in a high number of infections as compared to the transmission rate at the treatment centres. The study therefore suggests that infected individuals be sent to the treatment centres and proper treatment should also be carried out. The studies hence suggest that transmission of Ebola disease could be mitigated if proper measures are carried out at the treatment centres. Therefore, the implementation of clinical daily surveillance or prophylaxis after exposure (PEP) with favipiravir, health care worker training, and the provision of personal protective equipment (PPE) items may all contribute to the reduction of infection rates within Ebola treatment centres. By doing this, the Ebola disease will gradually die from the population. In the near future, the study will be extended to conduct an optimal control analysis into the Ebola disease by considering the results reported in this current study.

Declarations

Use of AI tools

The authors declare that they have not used Artificial Intelligence (AI) tools in the creation of this article.

Data availability statement

All data employed in this study for the parameter estimation have been duly referenced in this article.

Ethical approval (optional)

The authors state that this research complies with ethical standards. This research does not involve either human participants or animals.

Consent for publication

Not applicable

Conflicts of interest

The authors declare that they have no conflict of interest.

Author's contributions

I.K.A.: Conceptualization, Writing-Original draft preparation, Data Curation, Writing - Review & Editing, Methodology, Software, Formal Analysis. F.A.W.: Conceptualization, Writing Original draft preparation, Data Curation, Writing - Review & Editing, Methodology, Software, Formal Analysis. S.A.A.: Writing - Review & Editing, Methodology, Formal Analysis. G.O.A.: Writing-Original draft preparation, Methodology, Formal Analysis. All the authors were involved in the discussion of the entire results of this research and contributed to the final manuscript.

References

[1] Adu, I.K., Wireko, F.A., Nana-Kyere, S., Appiagyei, E., Osman, M.A.L. and Asamoah, J.K.K. Modelling the dynamics of Ebola disease transmission with optimal control analysis. *Modeling Earth Systems and Environment,* 10, 4731-4757, (2024). [CrossRef]

[2] Adu, I.K., Wireko, F.A., Osman, M.A.L. and Asamoah, J.K.K. A fractional order Ebola transmission model for dogs and humans. *Scientific African,* 24, e02230, (2024). [CrossRef]

[3] Gonzalez, A., Nikparvar, B., Matson, M.J., Seifert, S.N., Ross, H.D., Munster, V. and Bharti, N. Human movement and transmission dynamics early in Ebola outbreaks. *medRxiv,* (2023). [CrossRef]

[4] Savini, H., Janvier, F., Karkowski, L., Billhot, M., Aletti, M., Bordes, J. et al. Occupational exposures to Ebola virus in Ebola treatment center, Conakry, Guinea. *Emerging Infectious Diseases,* 23(8), 1380-1383, (2017). [CrossRef]

[5] Madelain, V., Nguyen, T.H.T., Olivo, A., De Lamballerie, X., Guedj, J., Taburet, A. and Mentré, F. Ebola virus infection: review of the pharmacokinetic and pharmacodynamic properties of drugs considered for testing in human efficacy trials. *Clinical Pharmacokinetics,* 55, 907-923, (2016). [CrossRef]

[6] Billioux, B.J., Smith, B. and Nath, A. Neurological complications of Ebola virus infection. *Neurotherapeutics,* 13(3), 461-470, (2016). [CrossRef]

[7] Adu, I.K., Wireko, F.A., Sebil, C. and Asamoah, J.K.K. A fractal-fractional model of Ebola with reinfection. *Results in Physics,* 52, 106893, (2023). [CrossRef]

[8] Thom, R., Tipton, T., Strecker, T., Hall, Y., Bore, J.A., Maes, P. et al. Longitudinal antibody and T cell responses in Ebola virus disease survivors and contacts: an observational cohort study. *The Lancet Infectious Diseases,* 21(4), 507-516, (2021). [CrossRef]

[9] Rugarabamu, S., Mboera, L., Rweyemamu, M., Mwanyika, G., Lutwama, J., Paweska, J. and Misinzo, G. Forty-two years of responding to Ebola virus outbreaks in Sub-Saharan Africa: a review. *BMJ Global Health,* 5(3), e001955, (2020). [CrossRef]

[10] Karaagac, B., Owolabi, K.M. and Pindza, E. A computational technique for the Caputo fractal-fractional diabetes mellitus model without genetic factors. *International Journal of Dynamics and Control,* 11, 2161-2178, (2023). [CrossRef]

[11] Wireko, F.A., Adu, I.K., Gyamfi, K.A. and Asamoah, J.K.K. Modelling the transmission be-

havior of Measles disease considering contaminated environment through a fractal-fractional Mittag-Leffler kernel. *Physica Scripta,*, 99, 075025, (2024). [CrossRef]

[12] Wireko, F.A., Adu, I.K., Sebil, C. and Asamoah, J.K.K. A fractal-fractional order model for exploring the dynamics of Monkeypox disease. *Decision Analytics Journal,* 8, 100300, (2023). [CrossRef]

[13] Nana-Kyere, S., Boateng, F.A., Jonathan, P., Donkor, A., Hoggar, G.K., Titus, B.D. et al. Global analysis and optimal control model of COVID-19. *Computational and Mathematical Methods in Medicine,* 2022, 9491847, (2022). [CrossRef]

[14] Qureshi, S. and Atangana, A. Fractal-fractional differentiation for the modeling and mathematical analysis of nonlinear diarrhea transmission dynamics under the use of real data. *Chaos, Solitons & Fractals,* 136, 109812, (2020). [CrossRef]

[15] Asamoah, J.K.K., Okyere, E., Yankson, E., Opoku, A.A., Adom-Konadu, A., Acheampong, E. and Arthur, Y.D. Non-fractional and fractional mathematical analysis and simulations for Q fever. *Chaos, Solitons & Fractals,* 156, 111821, (2022). [CrossRef]

[16] Alzahrani, E.O. and Khan, M.A. Modeling the dynamics of Hepatitis E with optimal control. *Chaos, Solitons & Fractals,* 116, 287-301, (2018). [CrossRef]

[17] Liana, Y.A. and Chuma, F.M. Mathematical modeling of giardiasis transmission dynamics with control strategies in the presence of carriers. *Journal of Applied Mathematics,* 2023, 1562207, (2023). [CrossRef]

[18] Eikenberry, S.E. and Gumel, A.B. Mathematical modeling of climate change and malaria transmission dynamics: a historical review. *Journal of Mathematical Biology,* 77, 857-933, (2018). [CrossRef]

[19] Byamukama, M., Kajunguri, D. and Karuhanga, M. Optimal control analysis of pneumonia and HIV/AIDS co-infection model. *Mathematics Open,* 3, 2450006, (2024). [CrossRef]

[20] Cetin, M.A. and Araz, S.I. Prediction of COVID-19 spread with models in different patterns: A case study of Russia. *Open Physics,* 22(1), 20240009, (2024). [CrossRef]

[21] Arik, I.A., Sari, H.K. and Araz, S.İ. Numerical simulation of Covid-19 model with integer and non-integer order: The effect of environment and social distancing. *Results in Physics,* 51, 106725, (2023). [CrossRef]

[22] Djiomba Njankou, S.D. and Nyabadza, F. Modelling the role of human behaviour in Ebola virus disease (EVD) transmission dynamics. *Computational and Mathematical Methods in Medicine,* 2022, 150043, (2022). [CrossRef]

[23] Rafiq, M., Ahmad, W., Abbas, M. and Baleanu, D. A reliable and competitive mathematical analysis of Ebola epidemic model. *Advances in Difference Equations,* 2020, 540, (2020). [CrossRef]

[24] Nazir, A., Ahmed, N., Khan, U., Mohyud-Din, S.T., Nisar, K.S. and Khan, I. An advanced version of a conformable mathematical model of Ebola virus disease in Africa. *Alexandria Engineering Journal,* 59(5), 3261-3268, (2020). [CrossRef]

[25] Rachah, A. and Torres, D.F.M. Mathematical modelling, simulation, and optimal control of the 2014 Ebola outbreak in West Africa. *Discrete Dynamics in Nature and Society,* 2015, 842792, (2015). [CrossRef]

[26] Singh, H. Analysis for fractional dynamics of Ebola virus model. *Chaos, Solitons & Fractals,* 138, 109992, (2020). [CrossRef]

[27] Farman, M., Akgül, A., Abdeljawad, T., Naik, P.A., Bukhari, N. and Ahmad, A. Modeling

and analysis of fractional order Ebola virus model with Mittag-Leffler kernel. *Alexandria Engineering Journal,,* 61(3), 2062-2073, (2022). [CrossRef]

[28] Adu, I.K. and Wireko, F.A. On SITR theoretical model of Ebola virus propagation with relapse and reinfection. *International Journal of Innovation and Development,* 1(3), (2023).

[29] Addai, E., Zhang, L., Preko, A.K. and Asamoah, J.K.K. Fractional order epidemiological model of SARS-CoV-2 dynamism involving Alzheimer's disease. *Healthcare Analytics,* 2, 100114, (2022). [CrossRef]

[30] Qureshi, A.I., Chughtai, M., Loua, T.O., Pe Kolie, J., Camara, H.F.S., Ishfaq, M.F. et al. Study of Ebola virus disease survivors in Guinea. *Clinical Infectious Diseases,* 61(7), 1035-1042, (2015). [CrossRef]

[31] Kengne, J.N. and Tadmon, C. Ebola virus disease model with a nonlinear incidence rate and density-dependent treatment. *Infectious Disease Modelling,* 9(3), 775-804, (2024). [CrossRef]

[32] MacIntyre, C.R. and Chughtai, A.A. Recurrence and reinfection-a new paradigm for the management of Ebola virus disease. *International Journal of Infectious Diseases,* 43, 58-61, (2016). [CrossRef]

[33] Rezapour, S., Asamoah, J.K.K., Hussain, A., Ahmad, H., Banerjee, R., Etemad, S. and Botmart, T. A theoretical and numerical analysis of a fractal-fractional two-strain model of meningitis. *Results in Physics,* 39, 105775, (2022). [CrossRef]

[34] Atangana, A. Fractal-fractional differentiation and integration: connecting fractal calculus and fractional calculus to predict complex system. *Chaos, Solitons & Fractals,* 102, 396-406, (2017). [CrossRef]

[35] Samet, B., Vetro, C. and Vetro, P. Fixed point theorems for α-ψ-contractive type mappings. *Nonlinear Analysis: Theory, Methods & Applications,* 75(4), 2154-2165, (2012). [CrossRef]

[36] Jiang, S., Zhang, J., Zhang, Q. and Zhang, Z. Fast evaluation of the Caputo fractional derivative and its applications to fractional diffusion equations. *Communications in Computational Physics,* 21(3), 650-678, (2017). [CrossRef]

[37] Padder, A., Almutairi, L., Qureshi, S., Soomro, A., Afroz, A., Hincal, E. and Tassaddiq, A. Dynamical analysis of generalized tumor model with Caputo fractional-order derivative. *Fractal and Fractional,* 7(3), 258, (2023). [CrossRef]

[38] Sikora, B. Remarks on the Caputo fractional derivative. *Minut,* 5, 76-84, (2023).

[39] Baba, I.A., Ahmed, I., Al-Mdallal, Q. M., Jarad, F. and Yunusa, S. Numerical and theoretical analysis of an awareness COVID-19 epidemic model via generalized Atangana-Baleanu fractional derivative. *Journal of Applied Mathematics and Computational Mechanics,* 21(1), 7-18, (2022). [CrossRef]

[40] Ahmed, I., Yusuf, A., Ibrahim, A., Kumam, P. and Ibrahim, M.J. A mathematical model of the ongoing coronavirus disease (COVID-19) pandemic: a case study in Turkey. *Science & Technology Asia,* 27(4), 248-258, (2022).[CrossRef]

[41] Hussain, A., Ahmed, I., Yusuf, A. and Ibrahim, M.J. Existence and stability analysis of a fractional-order COVID-19 model. *Bangmod International Journal of Mathematical and Computational Science,* 7, 102-125, (2021).

[42] Ahmed, I., Yusuf, A., Tariboon, J., Muhammad, M., Jarad, F. and Mikailu, B.B. A Dynamical and sensitivity analysis of the Caputo fractional-order Ebola virus model: implications for control measures. *Science & Technology Asia,* 28(4), 26-37, (2023).

[43] Granas, A. and Dugundji, J. *Fixed Point Theory*. Springer: New York, (2003). [CrossRef]

[44] Hyers, D.H. On the stability of the linear functional equation. *Proceedings of the National Academy of Sciences,* 27(4), 222-224, (1941). [CrossRef]

[45] Rassias, T.M. On the stability of the linear mapping in Banach spaces. *Proceedings of the American Mathematical Society,* 72, 297-300, (1978). [CrossRef]

[46] Gopal, K., Lee, L.S. and Seow, H.V. Parameter estimation of compartmental epidemiological model using harmony search algorithm and its variants. *Applied Sciences,* 11(3), 1138, (2021). [CrossRef]

[47] Asamoah, J.K.K., Owusu, M.A., Jin, Z., Oduro, F.T., Abidemi, A. and Gyasi, E.O. Global stability and cost-effectiveness analysis of COVID-19 considering the impact of the environment: using data from Ghana. *Chaos, Solitons & Fractals,* 140, 110103, (2020). [CrossRef]

[48] Asamoah, J.K.K., Jin, Z., Sun, G.Q., Seidu, B., Yankson, E., Abidemi, A. et al. Sensitivity assessment and optimal economic evaluation of a new COVID-19 compartmental epidemic model with control interventions. *Chaos, Solitons & Fractals,* 146, 110885, (2021). [CrossRef]

[49] Allahamou, A., Azroul, E., Hammouch, Z. and Alaoui, A.L. Modeling and numerical investigation of a conformable co-infection model for describing Hantavirus of the European moles. *Mathematical Methods in the Applied Sciences,* 45(5), 2736-2759, (2022). [CrossRef]

[50] Hamou, A.A., Rasul, R.R.Q., Hammouch, Z. and Özdemir, N. Analysis and dynamics of a mathematical model to predict unreported cases of COVID-19 epidemic in Morocco. *Computational and Applied Mathematics,* 41, 289, (2022). [CrossRef]

[51] Alla Hamou, A., Azroul, E. and Lamrani Alaoui, A. Fractional model and numerical algorithms for predicting COVID-19 with isolation and quarantine strategies. *International Journal of Applied and Computational Mathematics, Springer,* 7, 142, (2021). [CrossRef]

[52] Hamou, A.A., Azroul, E., Hammouch, Z. and Alaoui, A.L. A fractional multi-order model to predict the COVID-19 outbreak in Morocco. *Applied and Computational Mathematics,* 20(1), 177-203, (2020).

[53] Martcheva, M. *An Introduction to Mathematical Epidemiology* (Vol. 61). Springer: New York, (2015). [CrossRef]

[54] Asamoah, J.K.K. A fractional mathematical model of heartwater transmission dynamics considering nymph and adult amblyomma ticks. *Chaos, Solitons & Fractals,* 174, 113905, (2023). [CrossRef]

[55] Branda, F. and Maruotti, A. 2022 Uganda Ebola outbreak: Early descriptions and open data. *Journal of Medical Virology,* 95, e28344, (2023). [CrossRef]

[56] Branda, F., Mahal, A., Maruotti, A., Pierini, M. and Mazzoli, S. The challenges of open data for future epidemic preparedness: The experience of the 2022 Ebolavirus outbreak in Uganda. *Frontiers in Pharmacology,* 14, 1101894, (2023). [CrossRef]

[57] Worldometer. Population of Uganda, (2022). *World Population Prospects: The 2022 Revision, Frontiers Media SA* 1, (2022). https://www.worldometers.info/world-population/uganda-population.

[58] World Health Organization (WHO). Ebola Virus Disease, (2023). https://www.who.int/news-room/fact-sheets/detail/ebola-virus-disease.

[59] Castillo-Chavez, C. and Song, B. Dynamical models of tuberculosis and their applications. *Mathematical Biosciences and Engineering,* 1(2), 361-404, (2004). [CrossRef]

[60] Gemperli, A., Vounatsou, P., Sogoba, N. and Smith, T. Malaria mapping using transmission models: application to survey data from Mali. *American Journal of Epidemiology,* 163(3), 289-297, (2006). [CrossRef]

[61] Chen, J., Huang, J., Beier, J.C., Cantrell, R.S., Cosner, C., Fuller, D.O. et al. Modeling and control of local outbreaks of West Nile virus in the United States. *Discrete and Continuous Dynamical Systems-B*, 21(8), 2423-2449, (2016). [CrossRef]

[62] Ahmed, I., Kiataramkul, C., Muhammad, M. and Tariboon, J. Existence and sensitivity analysis of a Caputo fractional-order diphtheria epidemic model. *Mathematics,* 12(13), 2033, (2024). [CrossRef]

[63] Ahmed, I., Ibrahim, M.J., Abdullahi, M. and Saje, A.U. A mathematical analysis of a Caputo fractional-order cholera model and its sensitivity analysis. In *Modelling in Fractional-Order Systems with Applications in Engineering* (pp. 1-23). Lahore, Pakistan: Ptolemy Scientific Research Press, (2023).

Mathematical Modelling and Numerical Simulation with Applications (MMNSA)
(https://dergipark.org.tr/en/pub/mmnsa)